

IS SEEDLING ROOT ARCHITECTURE RELATED TO THE DEVELOPMENT OF SHOOT BIOMASS  
IN THE FIELD UNDER DROUGHT?  
LESSONS LEARNED FROM A REFERENCE SET OF 226 MAIZE INBRED LINES

A master thesis submitted to the Swiss Federal Institute of Technology Zurich  
(Department of Agricultural and Food Sciences)

for the degree of  
Master of Science ETH in Agroecosystem Science  
(MSc ETH Agr)

presented by

VANESSA SANDRA WEBER

B. Sc. (Subject Agricultural Sciences and Environmental Management)  
(Justus Liebig University Giessen, Germany)

Born February 12, 1985

citizen of Germany

Referee: Prof. Dr. P. Stamp

Co-Referee: Dr. A. Hund, Dr. R. Messmer

Supervision (CIMMYT): Dr. M. Zaharieva

Zurich, 22. July 2009

Auch das kleinste Ding  
hat seine Wurzel in der Unendlichkeit,  
ist also nicht völlig zu ergründen

Wilhelm Busch

1832 - 1908

Spricker

## II. Table of contents

<b>1</b>	<b>Summary .....</b>	<b>1</b>
<b>2</b>	<b>Introduction.....</b>	<b>3</b>
2.1	Food security and drought tolerance of maize.....	3
2.2	Indirect assessment of maize shoot production related to grain yield .....	4
2.3	Maize yield improvement influenced by root development under drought.....	5
2.4	Methods to research autotrophic and heterotrophic root growth .....	6
2.5	Objectives .....	8
<b>3</b>	<b>Material and Methods.....</b>	<b>9</b>
3.1	Generation of the reference set .....	9
3.2	Phenotyping of heterotrophic root growth in pouches.....	9
3.2.1	Seed disinfection and germination.....	9
3.2.2	Seed transfer into pouches .....	10
3.2.3	Scanning of the root system during 9 days after pouching.....	11
3.2.4	Image processing and differentiation between axile and lateral roots .....	12
3.2.5	Adjustment of the root length measured with a ruler (scan point 1) to the root length measured by WinRhizo.....	13
3.2.6	Determination of the total, axile and lateral root length .....	14
3.2.7	Calculation of the growth dynamics of axile and lateral roots.....	15
3.2.8	Distribution of the roots on the surface of the blotting paper .....	16
3.2.9	Measurement of photosynthetic parameters and shoot biomass .....	17
3.3	Phenotyping of the root growth during autotrophic stage in columns .....	17
3.4	Indirect measurement of the development of shoot biomass under drought stress in the field.....	18
3.4.1	Growth conditions at CIMMYT's experimental station Tlaltizapán.....	18
3.4.2	Measurement of canopy reflectance with a GreenSeeker device .....	20
3.5	Experimental design and statistical analysis.....	21
3.5.1	Experimental design and statistical analysis of root growth parameters assessed during heterotrophic stage in pouches.....	21
3.5.2	Experimental design and statistical analysis of the development of shoot biomass in the field under drought.....	23
3.5.3	Comparison among experiments .....	24
<b>4</b>	<b>Results .....</b>	<b>25</b>
4.1	Root growth during heterotrophic stage in pouches was mainly driven by the horizontal growth of axile roots .....	25
4.2	Elongation rate of individual axile and visible lateral roots improved the characterization of the genotypic root system.....	29
4.3	Seed size and vigor explained a small proportion of the variation of heterotrophic root and shoot growth .....	30
4.4	Root length during heterotrophic stage can be indirectly assessed with shoot parameters.....	31
4.5	Root traits in growth columns could related to total root length, $D_{95}$ and $\Phi_{PSII}$ measured in pouches .....	32
4.6	NDVI indicated the development and senescence of shoot biomass .....	36
4.7	Root development during heterotrophic stage related positively to early and negatively to late shoot biomass under drought .....	38
4.8	The development of axile roots during autotrophic stage related positively to shoot biomass under drought.....	40

<b>5</b>	<b>Discussion.....</b>	<b>43</b>
5.1	Heterotrophic root growth and distribution are best described by the ratio between lateral and axile root length, horizontal root length, $ER_{Ax(i)}$ and $k_{lat(v)}$ .....	43
5.2	Root growth parameters assessed during heterotrophic stage explained 20% of the root development during autotrophic stage .....	45
5.3	Operation efficiency of the photosystem II ( $\Phi_{PSII}$ ) measured in pouches related to the root development during autotrophic stage.....	46
5.4	NDVI precision was sensitive to plant density .....	47
5.5	Heterotrophic $ER_{Ax(i)}$ , $k_{lat}$ and horizontal root length related negatively related to late shoot biomass under drought.....	48
5.6	Autotrophic axile elongation rate positively related to shoot biomass under drought .....	50
<b>6</b>	<b>Conclusion .....</b>	<b>51</b>
<b>7</b>	<b>References .....</b>	<b>52</b>
<b>8</b>	<b>Appendix .....</b>	<b>55</b>

### III. List of Figures

Figure 1: Root length measured with a ruler (n=151) versus root length of the same plots measured by WinRhizo. The formula of the linear regression was used to adjust the root length measured with a ruler. ....	13
Figure 2: Design of the trials. Arrangement of 225 plots in 5 columns and 45 rows. ....	21
Figure 3: Field design of the drought stress experiment. Inbred lines were grouped according to three maturity classes and replicated three times (Rep 1-3) within these blocks (fields). Replications were subdivided into incomplete blocks, the size depended on the maturity class: 75 early lines (field 1617), 5 lines per block; 80 intermediate lines (field 1618), 10 lines per block; 80 late lines (field 1619), 10 lines per block. ....	23
Figure 4: Histogram of the square root transformed root length in diameter class distribution of the average of the genotypes. Superimposed on the histogram is a mixture model (solid) of the two normal components (short dashed) and a kernel estimated with Gaussian kernel and normal bandwidth (dashed). ....	26
Figure 5: Standardized (0 mean, 1 standard deviation) heterotrophic lateral and axile root length (cm).....	27
Figure 6: Standardized (0 mean, 1 standard deviation) root length in the border (vertical root length) and the upper third (horizontal root length) of the pouch. Genotypes in the upper right quarter (2, e.g. Entry 134) had a high horizontal to vertical root length, whereas genotypes in the lower right quarter (4, e.g. Entry 160) had a high vertical but low horizontal root length. The root growth in the different parts is indicated with the raster.....	28
Figure 7: Linear relationship between $\Phi_{PSII}$ measured 8 DAP and the elongation rate of roots during the V2 and the V6 stage (cm) measured in columns. ....	34
Figure 8: Development of the shoot biomass under drought stress over time indicated by NDVI. Error bars show the standard deviation.....	36
Figure 9: Pearson product-moment coefficients of determination of the measurement points 48, 77 and 97 DAS explaining the variation of NDVI over time. Filled symbols indicate significant correlations ( $p < 0.05$ ). ....	37
Figure 10: Slope estimates of standardized (0 mean, 1 standard deviation) TKW (g), leaf area ( $\text{cm}^2$ ), $ER_{Ax(i)}$ ( $\text{cm d}^{-1}$ ) $k_{lat(v)}$ ( $\text{cm d}^{-1}$ ) influencing NDVI. The slopes were the output of a multiple regression. Significant slopes ( $p < 0.05$ ) are indicated by filled symbols. The P-value as well as the adjusted and multiple $R^2$ of the model with the consistent parameters are shown in the table.....	39
Figure 11: Pearson product-moment coefficients between NDVI and total root length (pouch) as well as NDVI and the elongation rate of axile roots ( $D_{95(Ax)}$ Slp; column) in dependence of time. Significant correlations ( $p < 0.05$ ) are indicated with filled symbols.....	40
Figure 12: Slope estimates of standardized (0 mean, 1 standard deviation) total leaf area ( $\text{cm}^2/\text{day}$ ), $D_{95(Ax)}$ ( $\text{cm d}^{-1}$ ) and crown root number development influencing NDVI. The slopes were the output of a multiple regression. Significant slopes ( $p < 0.05$ ) are indicated by filled symbols. The P-value as well as the adjusted and multiple $R^2$ of the model with the consistent parameters are shown in the table. ....	41

#### IV. List of Tables

Table 1: Duration and amount of water applied with drip irrigation at different days after sowing (DAS).....	19
Table 2: Amount of fertilizers, herbicides and insecticides applied at different days after sowing (DAS). .....	19
Table 3: Mean values, standard deviation (sd) and heritability ( $h^2$ ) of best linear unbiased predictors (BLUPs) of root traits measured in pouches. Significant influences of run and climate chamber (ClCh) are indicated. ....	25
Table 4: Pearson product-moment correlation coefficients between root growth parameters to axile ( $ER_{Ax}$ ) and lateral elongation rate ( $k_{lat}$ ) as well as the elongation rate of individual axile roots ( $ER_{Ax(i)}$ ) and the elongation rate of visible lateral roots ( $k_{lat(v)}$ ). .....	29
Table 5: Pearson product-moment correlation coefficients between TKW, germination index (GI), percentage of germinated seeds (GP) to root and shoot development in pouches .....	30
Table 6: Mean values, standard deviation (sd) and heritability ( $h^2$ ) of BLUPs of the shoot traits in pouches. The number of inbred lines phenotyped for the different shoot traits is shown in brakes. Significant influences of run and climate chamber (ClCh) are indicated.....	31
Table 7: Pearson product-moment correlation coefficients between shoot and root development in pouches (22 repetitions of dry weight and $\Phi_{PSII}$ ; 223 repetitions of leaf and root parameters). .....	31
Table 8: Mean values of BLUPs of the root development (GCP-INRA subset) at the V2 stage in pouches and columns. Standard deviation is shown in brakes.....	32
Table 9: Pearson product-moment correlation coefficients of pouch and column parameters (n=22). Correlation coefficients of traits that should be comparable between pouches and columns are shaded in gray.....	35
Table 10: Pearson product-moment correlation coefficients of the intercept and slope of crown root angle to the development of shoot biomass over time. ....	42

#### V. Appendix

A 1: Macro programmed in Image J for inverting a colored picture to a black (background) and white (root) image. ....	55
A 2 Macro programmed in Image J for selecting and saving horizontal and vertical parts of the image .....	56

## 1 Summary

Drought stress is among the most important factors decreasing grain yield and shoot biomass of maize (*Zea mays L.*). Drought tolerant varieties with improved yield stability need to be developed to maintain global food security. Deeper rooting, achieved by altering root architecture, is a selectable trait towards this aim. Root architecture greatly determines the distribution of roots in soil and, thus, the plant's uptake efficiency of nutrients and water. This study aimed to assess the predictive value of the growth and distribution of axile roots at the seedling stage for later root development as well as for the development of shoot biomass under drought stress in the field.

For this purpose a set of 226 maize inbred lines was evaluated. The lines were selected by the Generation Challenge Program (GCP) to represent the world's diversity of tropical and subtropical maize. Within the framework of this thesis, the set was grown in growth pouches at ETH Zurich, to measure root traits, and at the International Maize and Wheat Improvement Center (CIMMYT) in Mexico, to measure the development of shoot biomass under drought stress in the field.

New protocols were developed to assess key parameters in growth pouches, i.e. the elongation rate of individual axile roots ( $ER_{Ax(i)}$ ) and the two dimensional distribution of roots on the blotting paper. The new parameters aimed to describe two basic features related to an increased rooting depth: stronger growth and more vertical orientation of the roots. A subset of 22 lines was used to compare these trait to those assessed during later developmental stages in sand substrate in growth columns (master thesis of Grieder 2008). With this the influence of the embryonic root system on the later autotrophic growth could be researched. The development of shoot biomass was indirectly assessed in the field by using the Normalized Difference Vegetation Index (NDVI) measured by a GreenSeeker<sup>TM</sup> sensor.

The major part of the heterotrophic root system measured in pouches was composed of axile roots, primarily located in the upper third of the pouch. The new parameter  $ER_{Ax(i)}$  described the potential growth of roots to greater depth better as the parameters used in previous studies.

Traits measured at the V2 stage in pouches showed no causal relationships to comparable traits measured in columns. These discrepancies indicated strong influences of seed effects (different seed lots were used) and of growth environments on early root development. Nevertheless, root growth during heterotrophic stage explained 18% of the variation in root development during autotrophic stage.

The  $ER_{Ax(i)}$  in pouches was positively associated with the early development of shoot biomass in the field emphasizing its role for plant establishment. This relationship turned negative during later stages of development disproving the positive impact of  $ER_{Ax(i)}$  on later water uptake under drought stress. However, the progress of rooting depth, including the development of crown roots, measured in columns was positively related to the development of shoot biomass throughout the season.

Neither the distribution of roots on the blotting paper nor the crown root angle measured in columns showed a significant relationship to the development of shoot biomass in the field.

The results suggest that early growth of embryonic roots is necessary for a successful plant establishment while later growth of crown roots into deeper soil layers enhances the development of shoot biomass under drought stress.



## **2 Introduction**

### **2.1 Food security and drought tolerance of maize**

Maize (*Zea mays* L.) is a staple food for vast numbers of people around the world (Camacho and Caraballo 1994). Global maize production was around 579 million tons in 1996, with the largest proportion (387 million tons) used for animal feed. The use for direct human consumption has remained stable around 100 million tons per year since 1988 (Calvo et al. 1999). The lack of water can be a major cause of famine and undernourishment, particularly in food-insecure rural areas of developing countries. The Food and Agriculture Organization of the United Nations (FAO) ranks drought as the “single most common cause of severe food shortages in developing countries” (FAO 2003). Bänziger et al. (1999) estimated that annually 24 million tons of maize yields are lost to drought. The incidence of drought will further increase due to global climate change (Campos et al. 2004), which will lead to a decrease in food supply. As a consequence, the Millennium Development Goal of 420 million undernourished people in 2015 is endangered by lower food supply and high food prices (FAO 2008).

Improved irrigation technology and drought tolerant crops can mitigate the impact of drought. Irrigation of maize fields is not sustainable because water resources for agronomic uses become more limiting (Boyer and Westgate 2004). Consequently the development of drought tolerant lines becomes increasingly important (Bruce et al. 2002). Selection for drought tolerance in maize is most promising at flowering, because maize is most susceptible to stress at this developmental stage (Campos et al. 2004). Secondary traits are used for the selection, because the selection based on grain yield alone is inefficient due to a decline in heritability under stress (Bolaños and Edmeades 1996; Monneveux et al. 2008). Secondary traits should be genetically associated with grain yield under drought, genetically variable, highly heritable, easy to measure, and stable over time (Campos et al. 2004; Monneveux et al. 2008).

Secondary traits for drought tolerance in maize are for example a short anthesis-silking-interval (ASI), reduced bareness, stay-green and visual scores for leaf rolling and leaf senescence (Edmeades et al. 1999, Bolaños and Edmeades 1996, Monneveux et al. 2008).

## **2.2 Indirect assessment of maize shoot production related to grain yield**

The shoot biomass production over time can be used to predict grain yield as it is positively correlated with yield of rice (Babu et al. 2003), maize (Inman et al. 2007) and wheat (Marti et al. 2007). The assessment of shoot biomass is very laborious because it has to be harvested, dried and weighted. As a result non-destructive biomass estimations like spectral reflectance indices (SRI) are useful for continuous shoot biomass estimation during the whole crop cycle (Marti et al. 2007). One of the most widely used SRI is the Normalized Difference Vegetation Index (NDVI) which relates the difference between near infrared reflectance and red wavelength reflectance with the reflectance of both wavelengths (Marti et al. 2007). The NDVI is more sensitive to changes in the crop canopy when the leaf area index is low. It becomes saturated when the crop canopy closes (Inman et al. 2008). Different studies showed that the development of shoot biomass (Marti et al. 2007), yield potential (Teal et al. 2006, Inman et al. 2007) and leaf area index (Marti et al. 2007) of maize could be accurately predicted with NDVI measured with a GreenSeeker™ sensor (GreenSeeker Hand-Held Data Collection and Mapping Unit, NTech Industries, Ukiah, CA, USA)

### **2.3 Maize yield improvement influenced by root development under drought**

Maize yield improvement is the result of increased interception of radiation and greater uptake of nutrients and water (Tollenaar and Wu 1999). Based on simulations, Hammer et al. (2009) concluded that changes in the architecture of root systems, which led to a better water capture by deeper roots, had a higher influence on enhanced plant growth, biomass accumulation and yield increase under high plant density than the change in canopy architecture and light capture. A better understanding of the structure and function of the root system is important for crop improvement in drought prone environments (Manschadi et al. 2006).

Maize has a fasciculated fibrous root system composed of primary, seminal and crown roots. During the first two weeks of heterotrophic development the embryonic primary and seminal roots represent the major portion of the seedling rootstock (Hochholdinger et al. 2004). Seminal roots arise at the mesocotyl-radicle junction and are important for water uptake in maize at emergence and establishment (Cahn 1989, Hill 2007). The number of seminal roots per seedling depends on the genotype and varies between 0 and 13. During the early post-embryonic development the lateral roots emerge from the primary and seminal roots (Hund et al. 2004). Lateral roots are the main entrance point for water and nutrients due to their branching capacity (McCully and Canny 1988). The branching leads to lateral roots of second, third and higher order (Hochholdinger et al. 2004). The late postembryonic root development is characterized by the development of shoot-borne crown and brace roots. Crown roots are distinguished by the node they arise from. The crown roots form the major part of the adult rootstock and are the basis for lodging resistance of the plants (Hochholdinger et al. 2004). Primary, seminal and crown roots are termed "axile" roots after the hierarchical system of Cahn (1989). The axile roots grow mainly vertically through the soil for reaching deep water sources.

The depth and intensity of rooting, elongation rate, water use efficiency and the timing of water extraction are researchable traits identified from measurements of germplasm grown under drought stress (Campos et al. 2004, Hund et al. 2009a).

#### **2.4 Methods to research autotrophic and heterotrophic root growth**

Although the lateral and axile roots represent an important part of the root system, their developmental morphology and morphological variations have rarely been studied (Ito et al. 2006). “The reason we know relatively little about root architecture is that it is difficult to observe, quantify, and interpret” (Lynch 1995). The difficulties concerning root observation promoted the development of various destructive and non-destructive investigative techniques (Böhm 1979). With non-destructive techniques like growth pouches the morphological changes of roots during the heterotrophic phase, defined as the growth of primary and seminal roots, can be observed (Ohdan et al. 1995, Hund et al. 2009b). The growth in pouches is usually assessed during the very early stage, which is mainly driven by seed reserves. The heterotrophic root growth in pouches ends at about the V2 stage which is the stage, when maize seed reserves begin to be exhausted and the carbohydrate supply from the leaves starts to dominate (Enns et al. 2006). The system permits the analysis of root geometry in two dimensions, including the distribution of roots in different layers and the measurement of root growth angles. Due to its simplicity the growth pouch system is suited for large experiments (Liao et al. 2004). Further it is possible to apply controlled stresses like desiccation (Ruta et al 2009), temperature, salt and nutrient stresses (Bonser et al. 1996, Liao et al. 2001).

The growth of primary, seminal and crown roots during the autotrophic phase, can be observed with columns by harvesting the root and shoot biomass at different time points. The columns allow a description of the root system at the time point of sampling (Böhm 1979). Additionally developmental root processes can be investigated if different time points are observed for selected genotypes (Liedgens et al. 2000). The problem is that the destructive sampling strategy is very laborious, which restricts the number of genotypes that can be evaluated.

The presented root observation systems were used in different studies concerning root length and drought tolerance of different genotypes. Bolaños et al. (1993) observed in large pots that the selection for drought tolerance reduced root biomass in the upper 50 cm. The data suggested that responses to selection in grain yield, ASI and harvest index were due to improved partitioning of biomass toward the female inflorescence at flowering. This was accompanied by a reduction in upper root growth which may compete with that of the developing ear (Bolaños et al. 1993). Additionally, the shifting biomass from the upper soil zones to deeper regions would enhance the chances of encountering new water resources (Bruce et al. 2002). As a result plant breeding for drought tolerance decreased horizontal but increased vertical root growth. Ruta et al. (2009) found QTL (Quantitative Trait Loci) for elongation rates of axile roots that responded to water stress. Additionally the authors found a QTL for constitutive increase in  $k_{lat}/ER_{Ax}$  co-located with a major QTL for the anthesis-silking-interval suggesting an involvement of root morphology in drought tolerance (Ruta et al. 2009). Thus the elongation rate seemed to be an interesting parameter which can be researched during the heterotrophic stage.

The results of studies conducted under drought stress indicate that a deep root system maintains a higher plant growth rate under drought stress (Hammer et al. 2009, Cutforth et al. 1985, Tollenaar and Wu 1999). As a result a root system with fewer lateral roots in the topsoil but thicker deep axile roots should be more suitable for drought avoidance (Hund et al. 2009a). The improved resource capture is further associated with increased leaf longevity (Tollenaar and Wu 1999). The influence of increasing root on the development of shoot biomass in the field was only predicted in the study of Schmidhalter et al. (1998), who observed for maize grown in pots for 18 days that the largest root diameter class increased at the expense of leaf elongation rate under drought.

As such drought tolerant plants tend to produce less biomass but are able to yield more under drought stress. The predictive value of the elongation rate of the roots and root distribution at early stages of development has yet to be determined.

There are at least two hypotheses how greater rooting depth may be achieved in maize:

- 1) According to Hund et al. (2009b) a strong axile root length in expense of the lateral roots leads to an increased root length. Thus genotypes with a prolific growth of axile roots during heterotrophic and autotrophic stage should be more drought tolerant than genotypes with more prolific development of lateral roots.
- 2) According to Hammer et al. (2009) a smaller root angle closer to vertical growth leads to a greater rooting root depth. Thus the genotypes with smaller root angle should be drought tolerant.

## **2.5 Objectives**

The aim of the study was to test for the two different hypotheses as cause for better development of plant biomass under drought stress i) an increase in the growth of axile roots and ii) an increase in vertical orientation of the axile roots. To achieve this, a representative sample of 226 temperate, tropical and subtropical maize inbred lines was characterized for the above traits under well watered conditions using growth pouches. The predictive value of these traits was tested by correlating them with comparable traits observed on a subset of 22 lines at later stages in growth columns (Grieder 2008) and with the development of shoot biomass of the whole set in the field under drought stress.

### **3 Material and Methods**

#### **3.1 Generation of the reference set**

The used material consisted of a reference set of 240 inbred lines adapted to temperate, tropical and subtropical climate derived from CIMMYT. The constitution of the reference set was part of the subprogram 1 of the Generation Challenge Program (GCP). The pedigree of the different entries can be requested from GCP or CIMMYT. The inbred lines were self fertilized in Mexico in summer 2008. Out of these, 224 produced enough seeds; the remaining 16 accessions were submitted to a second cycle of seed multiplication. The 224 lines were grouped, together with 5 CIMMYT control lines, in three maturity classes (early, intermediate and late) according to their flowering dates during seed production. 22 lines of the reference set were also used in the GCP-INRA panel evaluated by Christoph Grieder (2008). This subset is further called GCP-INRA subset.

#### **3.2 Phenotyping of heterotrophic root growth in pouches**

##### **3.2.1 Seed disinfection and germination**

For the trials, 221 genotypes of the composite set and 5 local control lines of CIMMYT were used. Ten Seeds per genotype were disinfected for two minutes with 2.5 % Sodiumhypoclorite (NaOCl). The seeds were rinsed 4 times with tap water. The sterilized seeds were imbibed and germinated in Petri dishes with deionised water over night at room temperature. The Petri dishes were covered with filter paper with a diameter of 70 mm (Macherey-Nagel AG, Oensingen, SO, CH). The seeds were covered with a wet paper towel for germination. The Petri dishes were filled with 2 mm water, closed and stored at 28°C in an incubator (Dexion, SRKäl Tetechnik + Partner, Winterthur, ZH, CH) for three days. The water was changed daily.

The number of germinated seeds was counted for calculating the germination index (*G*) and the percentage of germinated seeds.

The formula for the germination index of Hund et al. (2007) and Smith and Millet (1964) was amplified with the number of imbibed seeds multiplied with the days after imbibition (*DAI*):

$$GI = \frac{\sum (No. of seeds germinated on a given day \times DAI) \times No. of seeds germinated 4 DAI}{(number of imbibed seeds)^2} \quad [1]$$

The germination index varied from 0 to 10. 0 indicated that no seeds were germinated, whereas 10 indicated that all seeds germinated already on the first day after imbibition.

### **3.2.2 Seed transfer into pouches**

The germinated seeds were transferred to plastic pouches after 3 (run 1) to 4 (run 2) days after disinfection, which was done as described in Bonser et al. (1996). The pouches (22 x 30 cm) consisted of moistened blue blotting paper covered with an opaque polyethylene foil (Walser Kunststoffwerk AG, Buerglen, TG, CH, 0.5 mm 22 x 60 cm PE80, WA-1200). The foil was folded to obtain a pouch with the upper side closed. A hole of 5 mm diameter was cut in the middle of the upper side to allow the emergence of the coleoptile. On the front side a bulge of 10 mm diameter and 5 mm depth was molded 3 cm below the hole to keep the seed in place. The seed was placed on the moistened blue blotting paper under the bulge. The pouches were prepared one day before pouching and washed with hot tap water for two times to exclude negative effects of the paper (anchor paper 2008, St. Paul, MI, USA, 21 cm x 29.5 cm x 1 mm). The germinated seeds were transferred into pouches the day after.

The pouch was fixed with two standard paper clips (Jakob Maul GmbH, Bad König, DE), one on each side of the bulge. Afterwards the pouches were attached to a rod with two fold back clips. The exact time of pouching and the root length, measured with a ruler, for each plot was noted. The inclusion of root length at pouching was a new approach, not used in previous studies (compare to Ruta et al. 2009). The rods were placed upright into 5 containers (33 x 132 x 33 cm) each containing three blocks of pouches (Figure 2).



Hoagland solution was added after three days to the trials (Hoagland 1938). Two stock solutions were prepared:  $\text{KNO}_3$  (101 g/l, 10%),  $\text{Ca}(\text{NO}_3)_2$  (164 g/l, 16%) and  $\text{MgSO}_4$  (120.3 g/l, 12%) were mixed in stock solution 1.  $\text{KH}_2\text{PO}_4$  (136 g/l, 14%) was prepared as stock solution 2. 1.25 ml of stock solution 1 and 0.5 ml of stock solution 2 were added to 1 l deionised water for the final nutrient solution. The concentration of  $\text{KNO}_3$  and  $\text{Ca}(\text{NO}_3)_2$  was 2.5 mM. The final concentration for  $\text{MgSO}_4$  was 1 mM and for  $\text{KH}_2\text{PO}_4$  was 0.5 mM.

To avoid heating of the pouches the containers were covered with aluminum foil leaving a 2 cm wide opening through which the seed grew. The containers were placed in two growth chambers at a relative humidity of 60%, a photosynthetic active radiation of  $400 \pm 20 \mu\text{mol m}^{-2} \text{s}^{-1}$  and a photoperiod of 12 h. Two different climate chambers (Kli46, CMP 3246, Conviron, Winnipeg, MB, Canada; Kli 47, Hitachi SPS, Kälte3000 AG, GR, Switzerland) were used as two experiments were carried out simultaneously. The temperature was measured in 34 empty pouches at seed level during 9 days with a Hobo data logger (Hobo 4-Channel External, onset computer cooperation, MA, USA). The temperature in climate chamber 1 (Kli46) at the seed level was  $24.1^\circ\text{C}$  during the day and  $22.8^\circ\text{C}$  during the night. The day temperature in climate chamber 2 (Kli47) was  $21.5^\circ\text{C}$  and the night temperature  $19.2^\circ\text{C}$  at the seed level. The pH of the water at the end of the trials was 5.8.

### **3.2.3 Scanning of the root system during 9 days after pouching**

The root system of all genotypes was scanned three days after the seeds were transferred into the pouches with an A4 flatbed scanner (HP scanjet 4600, Hewlett-Packard Company, Palo Alto, CA, USA), as described in Hund et al. (2009b). Then the root system was scanned every three days. The root length at pouching served as first scan point. In total 4 scan points were taken.

The pouch was placed on a rack, opened, and axile roots that had grown out of the pouch were placed back on the blue blotting paper. The scanner was placed in 5 mm distance to the paper to avoid direct contact with the roots. The image was taken in RGB (red, green, blue) color mode with a resolution of 600 dpi ( $23.7 \text{ dots mm}^{-1}$ ) and a scanning area of 19 x 24 cm.

Images were saved with a custom software (PouchScan; ETH). Images were saved using the software. The basic information of each plot was saved in the image name as ETPAL code including information on Experiment, Treatment, Plot number, numbers of Axile (primary and seminal) roots and the existence of Lateral roots (0 = absent; 1 = present). Furthermore, the date and time of the measurement was saved. The files were stored as JPEG (Joint Photographic Experts Group) with the highest quality. The scanner was cleaned either with water or with alcohol after each scanning process.

### **3.2.4 Image processing and differentiation between axile and lateral roots**

Image processing described in Hund et al. (2009b) was improved by using ImageJ (ImageJ 1.41 o, Wayne Rasband, <http://rsb.info.nih.gov/ij>) instead of Photoshop 7.0 (Adobe Systems Inc., San Jose, CA, USA) followed by digital analysis in WinRhizo (WinRhizo™, Réagent Instruments, Montreal, QC, Canada). The advantage of ImageJ is that the image processing can be automatized. Additionally ImageJ does not change the Meta information of the pictures. ImageJ was used to reshape the colored image to black (root) and white (background), to remove image noise by applying the Gaussian Blur filter and to separate the roots from the background by applying an threshold tonal value (A 1). The resulting image was saved in JPEG format. In order to avoid poor image quality, all images were checked manually and severe image noise was removed manually in ImageJ with the command “makeRectangle” and “fill()”.

The program ExifTool (ExifTool 7.6, Phil Harvey, [www.sno.phy.queensu.ca](http://www.sno.phy.queensu.ca)) was used to change the Meta information of the pictures. This was necessary because WinRhizo can only read calibrated images. The Meta information was set at 1 dpi after scanning since PouchScan failed to store the appropriate Meta information of the true resolution (600 dpi). This information was changed to 600 dpi with ExifTool using the following command:

```
“exiftool . -xResolution=600 -yResolution=600  
-ResolutionUnit=inches -overwrite-original -k”.
```

WinRhizo was used to detect the “root length in diameter-class” distribution (RLDD) with an interval of 0.042 mm, the equivalent of one pixel. The debris removal filter of WinRhizo was set to remove objects with an area smaller than 0.03 cm<sup>2</sup> and a length/width ratio lower than 5.

### 3.2.5 Adjustment of the root length measured with a ruler (scan point 1) to the root length measured by WinRhizo

The ruler data were calibrated (Figure 1) to compare the root lengths measured with the ruler (1<sup>st</sup> scan point) with those determined using WinRhizo (2<sup>nd</sup>-4<sup>th</sup> scan point). This calibration was necessary, as the length of scanned roots was slightly overestimated due to image noise. The deviation between the two methods was estimated with a linear regression between the root length measured by a ruler ( $x$ ) and the root length measured by WinRhizo ( $y$ ):

$$y = 0.99x + 4.03 \quad [2]$$

The equation was derived by measuring root systems three days after pouching with one axile root but without lateral roots. The root length was overestimated by 4 cm because of noise in the image. This overestimation was constant through the trials as the slope of the linear regression was close to 1.

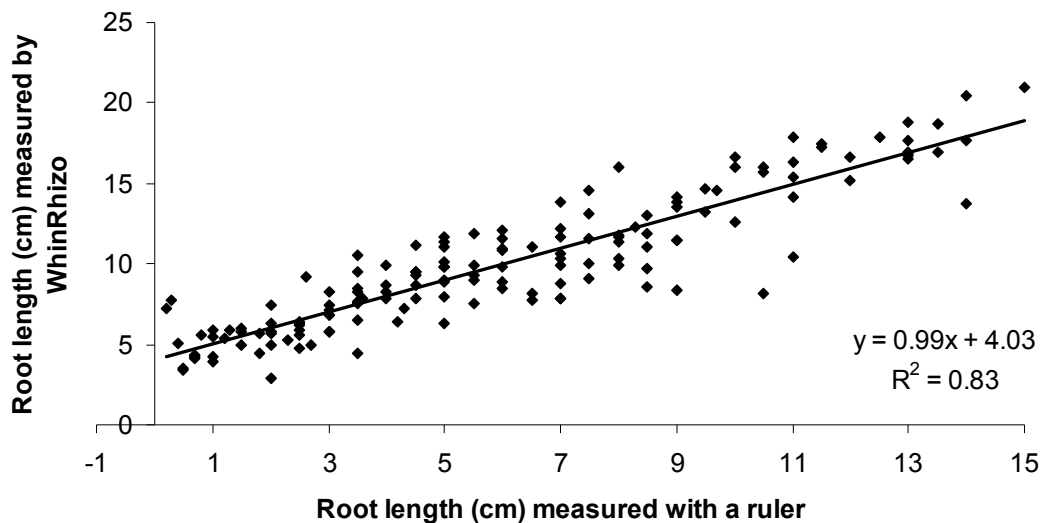


**Figure 1:** Root length measured with a ruler (n=151) versus root length of the same plots measured by WinRhizo. The formula of the linear regression was used to adjust the root length measured with a ruler.

### 3.2.6 Determination of the total, axile and lateral root length

The dynamics of the growth of axile and lateral roots was calculated using a two-step approach. First, the lengths of axile and lateral roots were extracted by fitting a mixture model to the RLDD of individual plots. Second, the growth of axile and lateral roots was computed by fitting linear models describing the temporal increase of these root types.

The mixture model of two normal distributions was fitted to the square-root transformed RLDD of the last image of each individual plot. The following log-likelihood function was used for the mixture model:

$$L(\pi, \mu_1, \sigma_1, \mu_2, \sigma_2) = \sum_{i=1}^n \log \left[ \frac{\pi}{\sigma_1} \phi \left( \frac{y_i - \mu_1}{\sigma_1} \right) + \frac{1 - \pi}{\sigma_2} \phi \left( \frac{y_i - \mu_2}{\sigma_2} \right) \right] \quad [3]$$

$\sigma$ : Standard deviation of each normal distribution  
 $\mu$ : Mean of each normal distribution  
 1= Lateral roots  
 2= Axile roots  
 $\pi$ : Proportion of the overall root length attributed to lateral roots  
 $y_i$  ( $i = 1, 2, \dots, n$ ): Diameter class (mm)

For fitting, the Nelder-Mead method implemented in the R-function `optim()` was used (R. 2.0.1, A language and environment, The R Development Core Team). The accuracy of the model was checked using a Q-Q plot.

The estimated parameters were used to generate the threshold (*TrSD*) and separate the RLDD into diameter classes representing lateral and axile roots.

$$TrSD = \mu_1 + \frac{(\mu_2 - \mu_1)}{1 + \frac{\sigma_2}{\sigma_1}} \quad [4]$$

$\sigma$ : Standard deviation of each normal distribution  
 $\mu$ : Mean of each normal distribution  
 1= Lateral roots  
 2= Axile roots

To avoid that poor adjustment of the mixture model had a strong influence on subsequent analyses, 10% of the outliers were identified based on standardized residuals and set as missing. Where the outliers were excluded the threshold was re-estimated.

The total root length (cm) was computed as the sum of lateral and axile roots (0.084 - 2.898 mm diameter).

Additionally the ratio between lateral and axile root lengths was computed. The axile and lateral root diameter was extracted of the diameter class representing the diameter class of the majority of axile and lateral roots, respectively.

With the number of axile roots (NoAx) during 9 days after pouching (DAP) the axile growth index (AGI) of the plots was computed:

$$AGI = \sum \left( \frac{Time}{\max(Time)} \times \frac{NoAx(DAP(n)) - NoAx(DAP(n-1))}{NoAx(9DAP)} \right) \quad [5]$$

### 3.2.7 Calculation of the growth dynamics of axile and lateral roots

The growth of individual axile roots was computed using equation 7, since the final length of axile roots includes the elongation rate of all axile roots and thus is usually strongly correlated with the number of axile roots. The length of individual axile roots  $L_{Ax(i)}$  was calculated as:

$$L_{Ax(i)} = \frac{x(t)}{n(t)} \quad [6]$$

$x(t)$ = Root length at time t after pouching

$n(t)$ = Number of axile roots developed at a given day (recorded in the ETPAL code)

According to the results of the mixed non-linear model the elongation rate of the axile roots ( $ER_{Ax}$ ) was modeled linearly and the elongation rate of the lateral roots ( $k_{lat}$ ) was modeled exponentially. The corresponding model to determine the elongation rate of axile roots ( $ER_{Ax}$ ) was:

$$L_{Ax}(t) = L_{Ax}(t_0) + ER_{Ax}t; \quad ER_{Ax} = \frac{L_{Ax}(t) - L_{Ax}(t_0)}{t} \quad [7]$$

$L_{Ax}(t)$ = Root length at time t after pouching

$L_{Ax}(t_0)$ = Root length at pouching

$t$  = Time after pouching

The elongation rate of individual axile roots ( $ER_{Ax(i)}$ ) was calculated similar to  $ER_{Ax}$  using  $L_{Ax(i)}$  instead of  $L_{Ax}$  as explaining variable.

The corresponding model for the lateral roots ( $k_{lat}$ ) was:

$$x(t) = x(t_0) \times e^{k_{lat}t}; \quad k_{lat} = \frac{\log(x(t) - x(t_0))}{\Delta t} \quad [8]$$

$x(t)$ = Root length of lateral roots at time t after pouching

$x(t_0)$ = Root length of lateral roots at pouching

$\Delta t$  = Lag between t and  $t_0$

The temporal change in the length of the population of lateral roots ( $L_{Lat}$ ) was used to estimate the rate constant of the lateral root elongation ( $k_{Lat}$ ). The  $k_{Lat}$  was computed using an altered protocol as the one described by Ruta et al. (2009). In the new protocol, the lag phase between pouching and the initiation of lateral roots was omitted from the analyses. This lag phase may be a cause of differences in germination and lead to inaccurate estimates of lateral root elongation. The information about the presence of lateral roots was recorded during scanning in the ETPAL code in the new protocol. Only those scan dates showing visible lateral roots were used for the regression analyses using the following equation:

$$L_{Lat}(t) = x(t_0) \times e^{k_{Lat}t}; \quad k_{Lat} = \frac{\log(L_{Lat}(t)) - \log(L_{Lat}(t_0))}{t} \quad [9]$$

$x(t)$ = Root length of visible lateral roots at time t after pouching  
 $x(t_0)$ = Root length of lateral roots at the first day of scanning

### 3.2.8 Distribution of the roots on the surface of the blotting paper

The basic parameters describing the distribution of roots in the pouches were assessed by dividing the images into three vertical and two horizontal sections using the command `makeRectangle()` in ImageJ (A 1).

The root length produced in the upper third (altitude=9.4 cm, latitude=20.17 cm) of the pouch was assigned as horizontal root length (cm). Additionally the ratio between horizontal and total root length was computed.

Using the three vertical images, the depth above which 95% of the roots were located ( $D_{95}$ ) and the proportion of the root length below half  $D_{95}$  (DR) were calculated using a modification of the protocol described by Hund et al. (2009a): Linear interpolations, instead of local fits, were used to extract the parameters. The DR is a modified deep root ratio with a plant-polynomial specific, flexible depth threshold to separate between deep and shallow roots.

The sum of the root lengths in the left and right border of the pouch was assigned as the vertical root length and was expressed as the proportion to total root length.

### 3.2.9 Measurement of photosynthetic parameters and shoot biomass

The date ( $D$ ) of leaf emergence ( $V_0$ ), the one-leaf-stage ( $V_1$ ) and two-leaf-stage ( $V_2$ ) were noted at the different scan days. The stages are defined according to the number of fully developed leaves with visible collars. If the two-leaf stage was not reached by a genotype the day of  $V_2$  was assigned as 10 days after pouching (DAP) which indicates that the leaf stage would only be reached after the trial.

A leaf growth index ( $LGI$ ) during 9 DAPS was computed as:

$$LGI = \frac{1 \times DV_0 + 2 \times DV_1 + 3 \times DV_2}{\text{number of developed leaves 9 days after pouching} \times (1 + 2 + 3)} \quad [10]$$

The leaf growth index varied up to 10. 10 indicated that no leaves were developed. The smaller the value, the faster the second-leaf stage was reached by the genotype.

The chlorophyll content of all genotypes was measured with a SPAD-meter (SPAD 502, Minolta Corporation, Ramsey, NJ, USA) previous to harvest. The chlorophyll content was measured four times at different sections of the second leaf. The operating quantum efficiency of the photosystem II ( $\Phi_{PSII}$ ) was measured with one repetition after 8 DAP in the INRA-GCP subset with a fluorometer (PAM-2000 fluorometer with leaf clip holder 20030-B, Walz, Effeltrich, DE). Leaf area of all genotypes was measured 9 DAP with a leaf area meter (Portable Area Meter LI-3000A, LICOR, inc., Lincoln, NE, USA) and the number of developed leaves per plant was counted.

The shoot and leaves of the INRA-GCP subset were dried at 60°C to constant weight for 3 days. The dry matter was determined by weighting.

### 3.3 Phenotyping of the root growth during autotrophic stage in columns

In the master thesis of Christoph Grieder, the 22 genotypes of the GCP-INRA subset were grown under well watered conditions in columns filled with sand-Seramix™ mixture. The plants were harvested at 2, 4 and 6 leaf stage with three replications. The maximum depth possible in columns was 80 cm. With the different harvest time points it was possible to depict the root development during autotrophic stage.

In the columns, the root length, the number of the development of crown roots as well as the angle and the diameter of crown roots were measured by Grieder (2008). For the measurement of root length, an indirect staining method was adapted and calibrated with the results obtained from WinRhizo. The development of crown roots was computed with the number of crown roots developed at the different developmental stages.

For the gravimetric set-point angle of the roots, vertical root growth was assigned by an angle of  $0^\circ$  and horizontal growth by  $90^\circ$ . The diameter of crown roots was measured from the first crown root. The axile roots in the columns represent the root length of primary, seminal and crown roots. The intercept (Int) and slope (Slp) of all parameters were computed by fitting a linear regression to the data. The intercept represented the heterotrophic stage whereas the slope represented the development during the autotrophic stage. For detailed description of the methods see Grieder (2008).

### **3.4 Indirect measurement of the development of shoot biomass under drought stress in the field**

#### **3.4.1 Growth conditions at CIMMYT's experimental station Tlaltizapán**

The plants were grown under drought stress and well watered conditions at CIMMYT's experimental station Tlaltizapán, Mexico ( $18^\circ 41' N$ ,  $99^\circ 10' W$ , 940 m asl elevation) during the dry (winter) season of 2009. In this study only the results of the drought stress experiment are shown, as the data of the well watered plots were not available by the end of the thesis. The soil was hilled up and the drought trials were drip irrigated (5 mm/hour) (Table 1). The application of fertilizer, herbicide and insecticide are shown in Table 2. The soil at this station is a calcareous vertisol (Isothermic Udic Pellustert), 1.3 to 1.8 m in depth, with a pH of 7.6 (Monneveux et al. 2005). Total water holding capacity in the top 1 m is 265 mm, of which about 100 mm is available to the crop (Bolaños and Edmeades 1993).



At 63 days after sowing (DAS), around 30 days before anthesis, the irrigation was stopped. Unfortunately, a hail incident occurred 15 days before anthesis with 47.7 ml precipitation, which relieved drought stress and damaged leaves.

**Table 1:** Duration and amount of water applied with drip irrigation at different days after sowing (DAS).

Irrigative time	DAS	Duration (h)	Amount of water applied (mm)
Germination	0	12	60
Elimination of the second plant/place	25	6	30
After hilling up the soil	50	6	30
Vegetative development	63	6	30
Rain and hail incident	78	4	47.4
Vegetative development	106	5	30

**Table 2:** Amount of fertilizers, herbicides and insecticides applied at different days after sowing (DAS).

Type	Application	DAS	Amount
Fertilization	N	0	85 kg/ha
Fertilization	P	0	70 kg/ha
Herbicide	Primagram	0	1 l/ha
Herbicide	Prowl	0	4 l/ha
Insecticide	Lorsban	13	2 lt/ha
Insecticide	Flash ultra	29	1 l/ha
Insecticide	Lorsban	29	1 l/ha
Insecticide	Flash ultra	39	1 l/ha
Insecticide	Lorsban	39	1 l/ha
Insecticide	Lorsban	47	2 l/ha
Herbicide	Doblete (Paraquat + Diquat)	95	2 l/ha
Herbicide	Lumax	95	1 l/ha
Fertilization	N	35-40	85 kg/ha

### 3.4.2 Measurement of canopy reflectance with a GreenSeeker device

The Normalized Difference Vegetation Index (NDVI) was measured using a GreenSeeker™ device (GreenSeeker Hand-Held Data Collection and Mapping Unit, NTech Industries, Ukiah, CA, USA). The sensor contains its own light source in the red (650±10 nm full width half magnitude (FWHM)) and near infrared (770±15 nm FWHM) bands, allowing for measurements independent of the sun light (Govaerts et al. 2007). The device measures the fraction of the emitted near infrared (*NIR*) and red light (*RED*) that is returned to the sensor (Marti et al. 2007). These fractions are used to compute the Normalized Difference Vegetation Index (*NDVI*):

$$NDVI = \frac{(NIR - RED)}{(NIR + RED)} \quad [11]$$

NIR= Fraction of emitted NIR radiation returned from the sensed area

RED= Fraction of emitted visible red radiation returned from the sensed area

NDVI was used as a proxy measure for shoot biomass in the field. Measurements were taken around midday in ten day intervals during the whole season. The head of the sensor was held approximately 0.5 m above canopy and oriented perpendicular to the row. Travel velocity was at slow walking speed. The sensor took approximately 1000 readings per second. The device averages the measurements between readings and computed NDVI at a rate of ten readings per second (Govaerts et al. 2007). At each time point, the bare soil surrounding the trials was measured as control value. This was necessary as the soil background can mask the reflectance of the crop canopy (Inman et al. 2008).

### 3.5 Experimental design and statistical analysis

#### 3.5.1 Experimental design and statistical analysis of root growth parameters assessed during heterotrophic stage in pouches

All data were analyzed as mixed effect models using the `asreml()` function in R (Butler 2006). The experimental design for parameters measured in pouches was an alpha lattice design with seven independent replications (runs), 1575 plots, 225 treatment factors (inbred lines, entry 167 did not germinate) and 45 plots per incomplete block (Figure 2). Within one block 15 pouches were placed. Successive scans (n=4) and root types were modeled as repeated measurements within plots. Each plot consisted of one pouch containing one plant.

	Column 1	Column 2	Column 3	Column 4	Column 5	
45	45	90	135	180	225	45
44	44	89	134	179	224	44
43	43	88	133	178	223	43
42	42	87	132	177	222	42
41	41	86	131	176	221	41
40	40	85	130	175	220	40
39	39	84	129	174	219	39
38	38	83	128	173	218	38
37	37	82	127	172	217	37
36	36	81	126	171	216	36
35	35	80	125	170	215	35
34	34	79	124	169	214	34
33	33	78	123	168	213	33
32	32	77	122	167	212	32
31	31	76	121	166	211	31
30	30	75	120	165	210	30
29	29	74	119	164	209	29
28	28	73	118	163	208	28
27	27	72	117	162	207	27
26	26	71	116	161	206	26
25	25	70	115	160	205	25
24	24	69	114	159	204	24
23	23	68	113	158	203	23
22	22	67	112	157	202	22
21	21	66	111	156	201	21
20	20	65	110	155	200	20
19	19	64	109	154	199	19
18	18	63	108	153	198	18
17	17	62	107	152	197	17
16	16	61	106	151	196	16
15	15	60	105	150	195	15
14	14	59	104	149	194	14
13	13	58	103	148	193	13
12	12	57	102	147	192	12
11	11	56	101	146	191	11
10	10	55	100	145	190	10
9	9	54	99	144	189	9
8	8	53	98	143	188	8
7	7	52	97	142	187	7
6	6	51	96	141	186	6
5	5	50	95	140	185	5
4	4	49	94	139	184	4
3	3	48	93	138	183	3
2	2	47	92	137	182	2
1	1	46	91	136	181	1
Plot						Row

**Figure 2:** Design of the trials. Arrangement of 225 plots in 5 columns and 45 rows.

An ANOVA (analysis of variance) was computed to test for influences on the root development. The run and climate chamber (CICH) were set as fixed factors. The random factors included in the model were the genotype (Entry), run, climate chamber (CICH), column and block:

Fixed: ~Run + CICH

Random: ~Entry + Entry:Run + Entry:CICH + Run:CICH + Run:CICH:Column +

Run:CICH:Column:Block

The plots without growing roots (n=128) and a leaf growth index of 10 (n=37) were excluded from the analysis.

The Best Linear Unbiased Predictors (BLUPs) were estimated and the broad-sense heritability ( $h^2$ ) was calculated as:

$$h^2 = \frac{\sigma_g^2}{\sigma_g^2 + \frac{1}{b}\sigma_e^2} \quad [12]$$

$\sigma_g^2$  = Genetic variance

$\sigma_e^2$  = Residual error variance

b = Number of replications

The mean based heritability of the root parameters were computed taking into account the genotypic, climate chamber and climate chamber to run variance.

The data were transformed, if the Q-Q plot or the Tukey-Anscombe plot indicated a strong divergence from normality or strong heteroscedasticity, respectively. Outliers were identified using Chauvenet's criterion and removed accordingly. The BLUPs were retransformed to the original scale if necessary.

### 3.5.2 Experimental design and statistical analysis of the development of shoot biomass in the field under drought

The field experiment was designed as randomized complete block design with 3 replications (Figure 3). The inbred lines were blocked in the field according to their maturity. 52 seeds were sown in each row to secure 26 plants per 5 m row (plot) with a 20 cm distance between plants and 40 cm distance between rows. Sowing date for the drought trials was 04.12.2008.

1618				1619				
Rep3	221	B23	B24	240	221	B23	B24	240
	201	B21	B22	220	201	B21	B22	220
	181	B19	B20	200	181	B19	B20	200
Rep2	161	B17	B18	180	161	B17	B18	180
	141	B15	B16	160	141	B15	B16	160
	121	B13	B14	140	121	B13	B14	140
	101	B11	B12	120	101	B11	B12	120
	81	B9	B10	100	81	B9	B10	100
Rep1	61	B7	B8	80	61	B7	B8	80
	41	B5	B6	60	41	B5	B6	60
	21	B3	B4	40	21	B3	B4	40
	1	B1	B2	20	1	B1	B2	20

1617				
Rep1	30	B1-6		1
	31	B7-12		60
Rep2	90	B13-18		61
	91	B19-24		120
Rep3	121	B25-30		150
	151	B31-36		180
	181	B37-42		210
	211	B43-45		225

**Figure 3:** Field design of the drought stress experiment. Inbred lines were grouped according to three maturity classes and replicated three times (Rep 1-3) within these blocks (fields). Replications were subdivided into incomplete blocks, the size depended on the maturity class: 75 early lines (field 1617), 5 lines per block; 80 intermediate lines (field 1618), 10 lines per block; 80 late lines (field 1619), 10 lines per block.

To test for influences on the shoot biomass an ANOVA was computed using the random factors genotype (entry), field, replication (rep) and block. The fixed factors included the intercept, only:

Fixed:~1

Random:~Entry + Field:Rep + Field:Rep:Block

The BLUPs were estimated and the broad-sense heritability ( $h^2$ ) was calculated by taking into account variance of the genotype. The data were transformed, outliers were identified and BLUPs were retransformed to the original scale if necessary, as described above.

### 3.5.3 Comparison among experiments

For the comparison of traits within and among experiments, a multiple correlation analysis after Pearson was calculated using the rcorr() function in R (R. 2.0.1, A language Environment, The R Development Core Team).

Correlations are measured in terms of strength of the relationship ( $R^2$  in %):

- a) >90 to 100 = very strong
- b) 75 to 90 = strong
- c) 50 to 75 = reasonably strong
- d) 25 to 50 = moderate
- e) <25 = weak
- f) <10 = very weak

The significant levels of the correlations are indicated as follows:

. =  $p < 0.05$       \*\* =  $p < 0.005$   
\* =  $p < 0.01$       \*\*\* =  $p < 0.001$

A correlation with a P-value larger than 0.05 was regarded as not significant.

## 4 Results

### 4.1 Root growth during heterotrophic stage in pouches was mainly driven by the horizontal growth of axile roots

The Q-Q-Plot of observed diameter measured by WinRhizo and the quartiles of the model output showed a normal distribution (data not shown). The mean total root length in the pouches was 120 cm with a standard deviation of 35 cm and a heritability of 0.8 (Table 3). The ratio between leaf area and root length was at mean 0.13 cm.

**Table 3:** Mean values, standard deviation (sd) and heritability ( $h^2$ ) of best linear unbiased predictors (BLUPs) of root traits measured in pouches. Significant influences of run and climate chamber (CICh) are indicated.

	Mean	Sd	$h^2$	Run	CICh
Total root length (cm)	119.52	34.52	0.8	***	***
Axile root length (cm)	90.9	27.96	0.8	**	***
Lateral root length (cm)	23.66	14.7	0.9		
Lateral root diameter	0.62	0.04	0.4		*
Axile root diameter	1.19	0.03	0.4	**	***
Horizontal root length (cm)	47.56	13.77	0.7	***	***
Ratio between horizontal root length and total root length (%)	37.03	4.75	0.6	*	***
DR (%)	38	3	0.5		***
$D_{95}$ (cm)	23.78	0.71	0.7	.	.
Ratio between leaf area and root length (cm)	0.13	0.03	0.9		

79% of the total root length was composed of axile roots and 21% was composed of lateral roots. The heritability of axile and lateral root lengths was 0.8.

The diameter class of axile roots ranged from 1.16 to 2.43 mm and of lateral roots from 0.16 to 1.42 mm (data not shown). The mean diameter of axile roots was 1 mm and of lateral roots 0.6 mm (Figure 4).

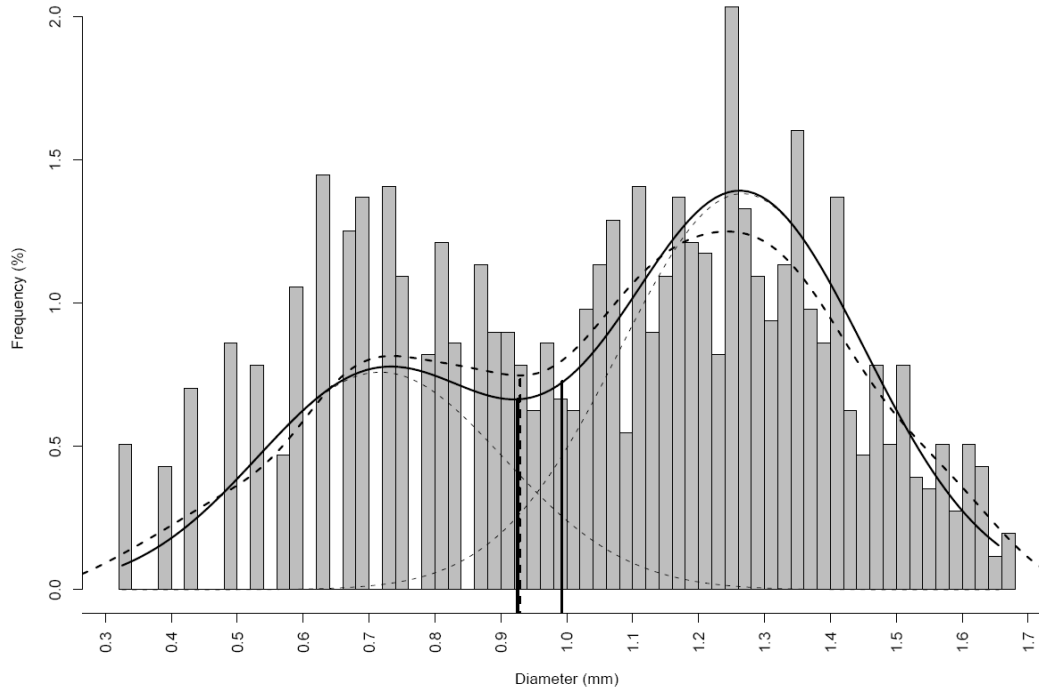


**Figure 4:** Histogram of the square root transformed root length in diameter class distribution of the average of the genotypes. Superimposed on the histogram is a mixture model (solid) of the two normal components (short dashed) and a kernel estimated with Gaussian kernel and normal bandwidth (dashed).

The axile root length was significantly influenced by the run and the climate chamber, whereas the lateral root length was not influenced by the two factors. The mean ratio between lateral and axile root ratio was 3:1. Thus the major part of the heterotrophic root system was composed of axile roots. The lateral and axile root length correlated positively ( $r=0.24^{***}$ ). On the other hand genotypes with a high axile root system did not always produce a high lateral root length as shown in (Figure 5). For most of the genotypes the causal relationship between increasing axile root to increasing lateral root length was observed (Figure 5; 2, 3). Some of the genotypes produced a high axile root length with a low lateral root length (Figure 5; 4) and vice versa (Figure 5; 1).



Thus, the ratio between lateral and axile root length can be used to characterize genotypes concerning their heterotrophic root system.

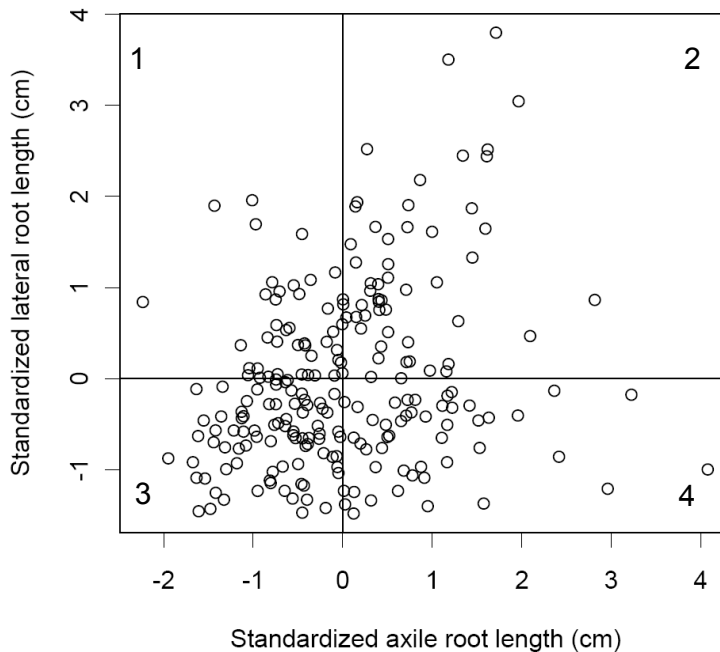


**Figure 5:** Standardized (0 mean, 1 standard deviation) heterotrophic lateral and axile root length (cm).

The  $D_{95}$  was reached at 24 cm, which was near the maximum of 25.45 cm achievable in pouches (Table 3). The  $D_{95}$  positively correlated with total root length ( $R^2=0.23^{***}$ ) with a heritability of 0.7. The proportion of the root length below half  $D_{95}$  (DR) was 38%. DR explained 14% of the total root length variation ( $r=0.37^{***}$ ) but the heritability ( $h^2=0.5$ ) of DR was low. DR and  $D_{95}$  can be used to describe the rooting depth reached by the different genotypes.

The vertical root length represented at mean 38% of the total root length. It explained 3% of the total root length variation ( $r=0.15$ ). The horizontal root length was 48 cm on average and represented 59% of the total root system. It correlated with total root length ( $R^2=0.71^{***}$ ). Thus, the highest proportion of root length was located in the upper third of the pouch.

The genotypes could be characterized by the proportion of vertical to horizontal root length (Figure 6). Some genotypes had a high vertical root to horizontal root length (Figure 6; 2), like entry 134 others a high horizontal and low vertical root length (Figure 6; 1), like entry 186.

Other genotypes had a high vertical and low horizontal root length (Figure 6; 4) like entry 160. Some of genotypes developed a low horizontal and vertical root length (Figure 6; 3), like entry 154. As a result, the horizontal and vertical root length can be used to characterize genotypes concerning their root distribution.

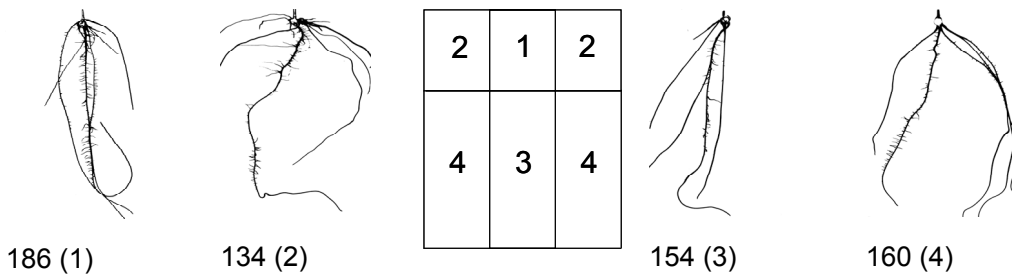
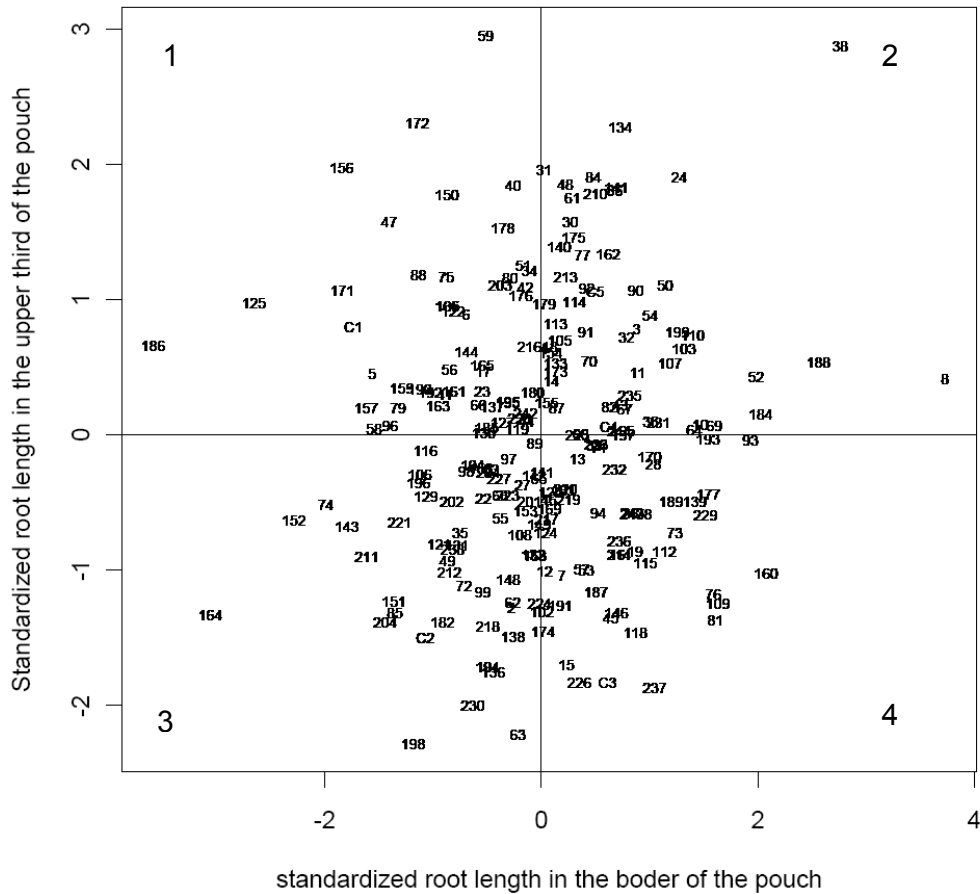


**Figure 6:** Standardized (0 mean, 1 standard deviation) root length in the border (vertical root length) and the upper third (horizontal root length) of the pouch. Genotypes in the upper right quarter (2, e.g. Entry 134) had a high horizontal to vertical root length, whereas genotypes in the lower right quarter (4, e.g. Entry 160) had a high vertical but low horizontal root length. The root growth in the different parts is indicated with the raster.

## 4.2 Elongation rate of individual axile and visible lateral roots improved the characterization of the genotypic root system

The elongation rate of lateral roots ( $k_{lat}$ ) as classically computed according to Ruta et al. (2009) and the elongation rate of visible lateral roots ( $k_{lat(v)}$ ) as computed here were positively correlated ( $r=0.72^{***}$ ) (Table 4). The same relationship was observed between the elongation rate of axile roots ( $ER_{Ax}$ ) and the elongation rate of individual axile roots ( $ER_{Ax(i)}$ ) ( $r=0.73^{***}$ ). The heritability of  $ER_{Ax(i)}$  was 0.6 and of  $k_{lat(v)}$  0.7. Taking into account only the growth of the visible lateral roots, the variation of lateral root length explained by  $k_{lat(v)}$  was reduced from 86% to 45%. Concerning the elongation rate of axile roots, the calculation for individual axile roots led to a significant negative relationship with the number of developed axile roots and the axile root index. When the whole elongation rate of axile roots was taken into account this relationship was positive. Thus it appears that the elongation rate of individual axile roots decreased with increasing number of axile roots. Taking only individual axile roots into account, the variation of axile root length explained by  $ER_{Ax}$  decreased from 98% to 73%. As the inclusion of visible lateral and individual axile roots improved the interpretation of genotypic system, only these parameters were used for further analysis.

**Table 4:** Pearson product-moment correlation coefficients between root growth parameters to axile ( $ER_{Ax}$ ) and lateral elongation rate ( $k_{lat}$ ) as well as the elongation rate of individual axile roots ( $ER_{Ax(i)}$ ) and the elongation rate of visible lateral roots ( $k_{lat(v)}$ ).

	$k_{lat}$ ( $cm\ d^{-1}$ )	$k_{lat(v)}$ ( $cm\ d^{-1}$ )	$ER_{Ax}$ ( $cm\ d^{-1}$ )	$ER_{Ax(i)}$ ( $cm\ d^{-1}$ )
Total root length (cm)	0.61 ***	0.57 ***	0.9 ***	0.62 ***
Axile root length (cm)	0.24 ***	0.33 ***	0.99 ***	0.73 ***
Lateral root length (cm)	0.93 ***	0.67 ***	0.27 ***	0.1
DR (%)	0.22 **	0.34 ***	0.33 ***	0.23 ***
$D_{95}$ (cm)	0.41 ***	0.39 ***	0.43 ***	0.37 ***
Ratio between lateral and axile root length	0.7 ***	0.37 ***	-0.27 ***	-0.3 ***
Number of developed axile roots	0.24 ***	0.13	0.43 ***	-0.23 ***
Axile root index	0.04	-0.01	0.09	-0.23 ***

### 4.3 Seed size and vigor explained a small proportion of the variation of heterotrophic root and shoot growth

The average thousand kernel weight (TKW) was 248.31 g ( $\pm 45.30$  g) (Table 5). The germination index (GI) of the genotypes was 5 ( $\pm 2.3$ ) and the average percentage of germinated seeds (GP) was 73% ( $\pm 23\%$ ). The heritability of GI and GP was 0.9.

TKW, GI and GP were not related with the exception of the axile root index, the vertical root length,  $ER_{Ax(i)}$ , DR,  $D_{95}$ ,  $\Phi_{PSII}$  and the ratio between leaf area and total root length (data not shown). Axile root index and the ratio between leaf area and total root length were the most reliable root parameters measured as the variability and heritability of these parameters was highest.

The highest correlation with TKW was observed for the total dry weight ( $R^2=0.23$ ) (Table 5). Only 12% of the total root length variation could be explained by TKW. Thus seed size could not explain more than 80% of root and 70% of shoot variation measured in pouches. GI and GP correlated slightly with the number of developed leaves ( $R^2=0.08$ ).

**Table 5:** Pearson product-moment correlation coefficients between TKW, germination index (GI), percentage of germinated seeds (GP) to root and shoot development in pouches

	TKW (g)	GI	GP
Leaf growth index	-0.18 *	-0.19 *	-0.18
No. of developed leaves	0.26***	0.28***	0.29***
Total leaf area (cm <sup>2</sup> )	0.48***	0.18	0.2 *
SPAD	0.19*	-0.01	0.03
Total dry weight (mg)	0.48 .	0.22	0.21
Total root length (cm)	0.35***	0.23***	0.26***
Axile root length (cm)	0.32***	0.26***	0.27***
Lateral root length (cm)	0.22***	0.12	0.15
Horizontal root length (cm)	0.34***	0.22 **	0.23***
Vertical root length (%)	0.06	0.13	0.1
DR (%)	0.17	-0.01	0
$D_{95}$ (cm)	0.13	-0.14	0.18
$ER_{Ax(i)}$ (cm d <sup>-1</sup> )	0.04	0.16	0.15
$k_{lat(v)}$ (cm d <sup>-1</sup> )	0.24***	-0.04	-0.02
Ratio between lateral and axile root length	-0.16	-0.21**	-0.2**
No. of developed axile roots	0.38***	0.15	0.18

#### 4.4 Root length during heterotrophic stage can be indirectly assessed with shoot parameters

The genotypes produced in pouches a total dry weight of 52 mg (Table 6). 31% of the total dry weight was shoot and 67% leaf biomass. The variation of shoot and photosynthesis parameters was high with the exception of the number of developed leaves and leaf growth index. The heritability was with 0.8 highest for leaf area, the number of developed leaves and SPAD. All root parameters were positively correlated with shoot traits and photosynthesis measured in pouches (Table 7). Above all total dry weight and leaf area positively can be used to indirectly assess the total, axile and lateral root length and development.

**Table 6:** Mean values, standard deviation (sd) and heritability ( $h^2$ ) of BLUPs of the shoot traits in pouches. The number of inbred lines phenotyped for the different shoot traits is shown in brakes. Significant influences of run and climate chamber (CICH) are indicated.

	Mean	Sd	$h^2$	Run	CICH
Total dry weight (mg) (n=22)	52.36	7.23	0.7		***
Leaf growth index (n=223)	3.04	0.24	0.7	***	***
No. of developed leaves 9DAP (n=223)	2.67	0.23	0.8	.	*
Total leaf area (cm <sup>2</sup> ) 9DAP (n=223)	15.64	3.59	0.8		***
$\Phi_{PSII}$ (n=22)	0.61	0.04	0.6		
SPAD (n=22)	22.71	3.03	0.8	*	

**Table 7:** Pearson product-moment correlation coefficients between shoot and root development in pouches (22 repetitions of dry weight and  $\Phi_{PSII}$ ; 223 repetitions of leaf and root parameters).

	No. of developed leaves	Leaf growth index	Total leaf area (cm <sup>2</sup> )	Total dry weight (mg)	$\Phi_{PSII}$	SPAD
Total root length (cm)	0.2 **	-0.18	0.52 ***	0.65 ***	0.43 .	0.25 ***
Axile root length (cm)	0.18	-0.15	0.45 ***	0.67 ***	0.44 .	0.18 *
Lateral root length (cm)	0.15	-0.17	0.37 ***	0.27	0.17	0.22 ***
Axile root index	-0.17	0.01	0.01	0.6 **	0.34	0.18
No. developed axile roots	0.02	-0.09	0.3 ***	0.61 **	0.4	0.22 **
Ratio between leaf area and root length (cm)	0.31 ***	-0.11	0.39 ***	-0.07	-0.2	-0.24 ***
Ratio between lateral and axile root length	0.03	-0.04	0.11	-0.25	-0.19	0.12
Ratio between lateral and axile root length Slp	-0.1	0.05	-0.21 **	-0.6 **	-0.19	-0.01
$k_{lat(v)}$ (cm d <sup>-1</sup> )	0.06	-0.12	0.29 ***	0.29	0.14	0.14
$ER_{Ax(i)}$ (cm d <sup>-1</sup> )	0.1	-0.07	0.24 ***	0.45 .	0.29	0.04
Horizontal root length (cm)	0.17	-0.16	0.5 ***	0.56 *	0.26	0.19 *
DR (%)	0.04	-0.03	0.3 ***	0.4	0.2	0.06
D <sub>95</sub> (cm)	0.2 **	-0.18	0.4 ***	0.35	0.33	0.15

#### 4.5 Root traits in growth columns could related to total root length, $D_{95}$ and $\Phi_{PSII}$ measured in pouches

Similar traits measured at the two-leaf stage in columns and pouches should be directly comparable. These traits are the diameter of the roots, DR,  $D_{95}$  and leaf area (Table 8).

The diameter of the crown roots from the second internodes (first crown root) measured in growth columns was in the range of lateral root diameter measured in pouches. The root length at the two-leaf stage in pouches was 4 times higher than the total root length developed in pouches. This indicated a strong effect of the growth environment on root morphology.

**Table 8:** Mean values of BLUPs of the root development (GCP-INRA subset) at the V2 stage in pouches and columns. Standard deviation is shown in brakes.

	Pouch	Column
Total root length (cm)	128.69 (35)	527.55 (340)
$D_{95}$ (cm)	23.77 (0.9)	17.37 (3)
DR (%)	0.38 (0.03)	0.25 (0.04)
Axile root diameter (mm)	1.19 (0.03)	-
Lateral root diameter (mm)	0.62 (0.04)	-
Crown root diameter (mm)	-	0.69 (0.08)
Total leaf area (cm <sup>2</sup> )	17.25 (4)	18.57 (21)

We used correlations among comparable traits measured in pouches and growth columns to estimate the heritability of the traits.

- l) Heterotrophic root length in pouches explained 18% of the elongation rate of the roots in columns

There was no relationship between the total root length measured in pouches and the root length measured at the two-leaf stage in columns (Table 9). The axile and lateral root lengths as well as the elongation rate of axile and lateral roots measured in pouches were neither significantly correlated with the elongation rate of the roots nor with the development of axile roots measured in columns. Further, root length and root development measured in pouches were not significantly correlated with the development of axile roots in columns. Additionally, the diameter of axile or lateral roots measured in pouches was not correlated to the crown root diameter measured in columns. However, heterotrophic root length explained 18% of the elongation rate of the roots during autotrophic stage.

II) Heterotrophic root growth can predict autotrophic rooting depth, root distribution and root diameter

A couple of traits were measured in the pouches that may be directly or indirectly related to rooting depth and root distribution in growth columns. The  $D_{95}$  and DR measured in pouches did not correlate with the same traits at the V2 stage in columns. However,  $ER_{Ax(i)}$  positively correlated with the autotrophic development of  $D_{95}$  ( $R^2=0.21$ ), what indicated that a greater growth velocity of axile roots in pouches led to greater rooting depth in the columns. The leaf area ( $R^2=0.25$ ) and  $\Phi_{PSII}$  ( $R^2=0.35$ ) had a greater positive influence on  $D_{95}$  in columns than  $ER_{Ax(i)}$ . Additionally, the axile (ns) and lateral root diameter measured in pouches were negatively correlated with the development of  $D_{95}$  in columns ( $R^2=0.19$ ).

III) Root distribution in pouches can not reliable describe gravitropic set point angles of crown roots in growth columns

The relationship between the distribution of roots on the blotting paper and the angle of the crown roots from the first tier in growth columns was weak to moderate. There was a negative correlation between DR and the angle of the crown roots from the first tier ( $R^2=0.27$ ). Thus a greater proportion of roots in the upper half of the root system in the pouch were related to a more horizontal root growth in columns. However, the heritability of DR was comparably low making it questionable that the trait is reliable for indirect selection for crown root angle. The relationship between vertical root length in the border of the pouch and crown root angle measured in columns was positive ( $r=0.15$ ) but not significant.

IV) Heterotrophic shoot growth and photosynthesis related to autotrophic shoot development

Leaf area measured at the two-leaf stage in pouches was not significantly related to the intercept of leaf area measured at the two-leaf stage in columns. However the total leaf area measured at the two-leaf stage (pouch) positively correlated with the slope of leaf area development between the two- and six-leaf stage (columns,  $R^2=0.26$ ). SPAD measured at the two-leaf stage in pouches was negatively correlated to the intercept of leaf area at the two-leaf stage measured in columns ( $R^2=0.25$ ).

V) Photosynthetic performance in pouches was the trait most strongly related to traits measured in growth columns

The operation quantum efficiency of the photosystem II measured at the V2 stage in pouches was positively correlated to the elongation rate of the roots ( $R^2=0.66$ ) (Figure 7),  $D_{95}$  ( $R^2=0.34$ ) and leaf area development ( $R^2=0.27$ ) in columns. The correlation between  $\Phi_{PSII}$  measured 8 DAP and root length increase in columns was twice as high as the relationship between root lengths in the two systems (Table 9). As such,  $\Phi_{PSII}$  was related to the root development during heterotrophic stage and autotrophic stage.

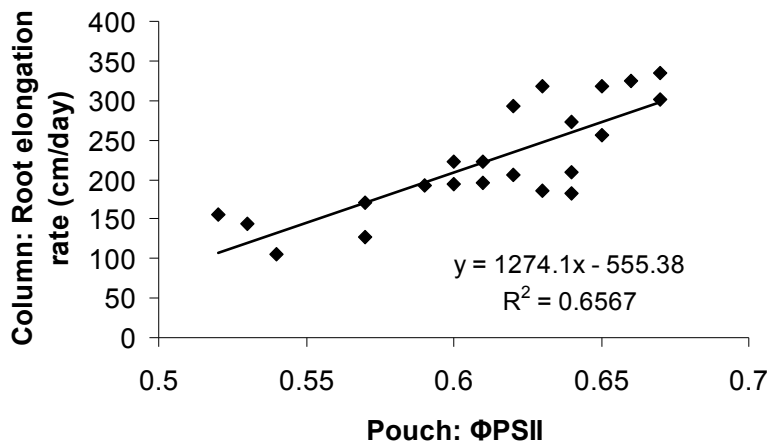


**Figure 7:** Linear relationship between  $\Phi_{PSII}$  measured 8 DAP and the elongation rate of roots during the V2 and the V6 stage (cm) measured in columns.

In total it can be concluded that no causal relationship between traits measured at the two-leaf stage in pouches and columns was found. On the other hand total root length,  $D_{95}$ , leaf area and  $\Phi_{PSII}$  could explain the variation of the slope of the different root and shoot traits measured during autotrophic root stage to some extend.



**Table 9:** Pearson product-moment correlation coefficients of pouch and column parameters (n=22). Correlation coefficients of traits that should be comparable between pouches and columns are shaded in gray.

Pouch \ Column	Total root length (cm) Slp	Total root length (cm) Int	D <sub>95</sub> (cm) Slp	D <sub>95</sub> (cm) Int	DR (%) Slp	DR (%) Int	Crown root number Slp	Crown root number Int	Crown root diameter (mm) Slp	Crown root diameter (mm) Int	Crown root angle (°) Slp	Crown root angle (°) Int	Leaf area (cm <sup>2</sup> ) Slp	Leaf area (cm <sup>2</sup> ) Int
Total root length (cm)	0.41	-0.02	0.34	-0.06	0.26	-0.1	0.04	0.02	0.21	-0.23	0.29	-0.13	0.31	-0.23
Axile root length (cm)	0.34	-0.01	0.4	-0.1	0.31	-0.16	0.13	0.12	0.17	-0.15	0.34	-0.19	0.38	-0.29
Lateral root length (cm)	0.25	0	0	0.02	0.02	0.07	-0.14	-0.11	0.1	-0.23	0.05	-0.04	-0.05	0.03
Axile root index	0.32	-0.17	0.16	-0.08	0.35	-0.2	0.26	-0.09	-0.34	0	0.16	-0.25	0.04	-0.1
No. of developed axile roots	0.24	-0.15	0.04	0.02	0.06	0.08	0.39	0.25	-0.33	-0.06	0.33	-0.36	-0.02	-0.08
Ratio between lateral and axile root length	0.01	-0.05	-0.19	0	-0.21	0.19	-0.19	-0.25	0.05	-0.11	-0.08	0.08	-0.24	0.19
Ratio between lateral and axile root length Slp	-0.14	-0.09	-0.19	-0.03	-0.26	0.13	-0.2	-0.26	-0.06	0.17	-0.26	0.12	-0.24	0.16
k <sub>lat(v)</sub> Slp	0.12	0.06	-0.09	0.17	0.12	0.16	-0.14	-0.13	-0.12	-0.33	0.14	-0.17	0.08	-0.07
ER <sub>Ax(i)</sub> Slp	0.27	0.14	0.46	-0.21	0.41	-0.25	-0.12	0.02	0.48	-0.2	0.25	-0.03	0.48	-0.29
D <sub>95</sub> (cm)	0.34	-0.34	0.06	0.04	-0.05	0.24	0.16	0.23	0.01	-0.56 *	0.28	-0.28	0.15	-0.36
DR (%)	0.07	0	0	0.07	0.01	0.21	-0.06	-0.12	-0.19	-0.15	0.17	-0.52	-0.01	-0.25
Horizontal root length (cm)	0.22	-0.05	0.08	-0.17	0.07	-0.03	0.27	0.03	0.03	-0.02	0.37	0.01	-0.01	-0.02
Axile root diameter (mm)	-0.24	0.04	-0.34	-0.19	-0.19	0.24	0.02	0.01	0.01	0.22	0.11	0.17	-0.36	0.36
Lateral root diameter (mm)	-0.31	0.06	-0.44	-0.03	-0.25	0.2	-0.17	-0.18	0	0.07	0.05	0.17	-0.44	0.41
Total leaf area (cm <sup>2</sup> )	0.39	0.02	0.5	-0.09	0.31	0.02	-0.07	0.11	0.15	-0.02	0.3	-0.05	0.51	-0.16
Total dry weight (mg)	0.34	0.17	0.31	-0.06	0.39	-0.03	-0.02	0.05	0.08	0.14	0.38	-0.16	0.32	0.01
SPAD	0.4	-0.13	0.41	0.35	0.04	0.11	0.07	-0.26	0.12	-0.17	-0.15	-0.28	0.26	-0.5
Φ <sub>PSII</sub>	0.81***	-0.3	0.59**	0.19	0.08	0.12	0.02	-0.09	0.25	-0.03	-0.04	-0.1	0.52	-0.31

#### 4.6 NDVI indicated the development and senescence of shoot biomass

The germination was predictive for GreenSeeker data in the field when plots with a low proportion of emerged plants were included in the analysis. The number of plants per plot correlated with all measured NDVI over time ( $r=0.3-0.4^{**}$ ). When plots with a proportion of less than 50% established plants were excluded from the analysis, this correlation disappeared. Consequently, the relationship between NDVI and the percentage of germinated seeds was due to 29 plots, which represented 15 inbred lines with a low percentage of germinated seeds and thus with an uneven plant stand in the field. These 29 plots were removed from the analysis. Mean biomass production indicated by NDVI increased in the drought trial until 82 DAS and decreased afterwards until 117 DAS (Figure 8). Anthesis was at mean 93 DAS (early: 86 DAS, intermediate: 94 DAS, late: 100 DAS) and silking at 99 DAS (early: 90 DAS, intermediate: 99 DAS, late: 106 DAS). Thus the development of shoot biomass increased until anthesis. Afterwards NDVI depicted the leaf senescence of the plants. The difference between maturity groups was not significant. Therefore the NDVI development of the whole population is shown in Figure 8. The hail incident (78 DAS) was between the third and fourth measuring point. The heritability was around 0.8 for all NDVI measurement points.

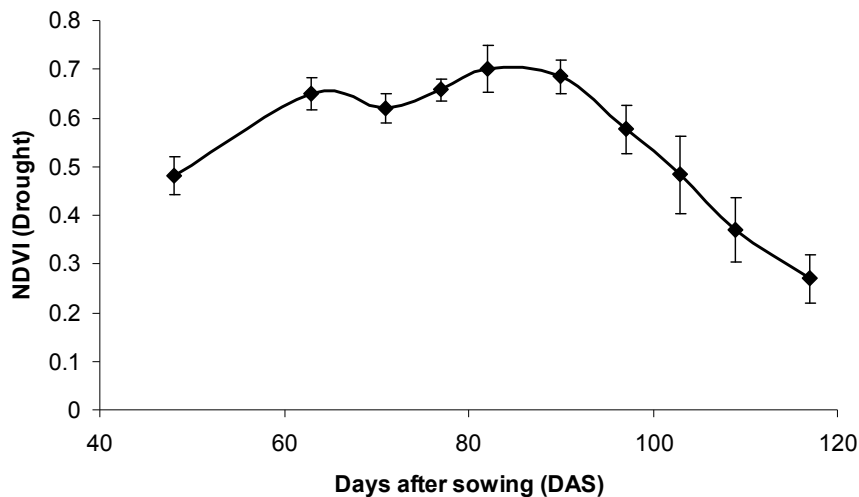


**Figure 8:** Development of the shoot biomass under drought stress over time indicated by NDVI. Error bars show the standard deviation.

The different measurement points of NDVI in the field were positively correlated with one another ( $R^2 = 0.04-83\%$ , data not shown). Thus the shoot biomass at the beginning of the season can predict shoot biomass later in the season to some extent. The coefficient of determination between the different measurement points was computed to assess the appreciation of the different measurement points. The result was that the measurement at 48 DAS can be used to predict early plant growth before anthesis (Figure 9). The measurement point at 48 DAS explained more than 23% of the variation until 77 DAS. The measurement 77 days after sowing could be used to predict the development of shoot biomass until and during male (93 DAS) and female flowering (99 DAS). The measurement 97 DAS could be taken to measure senescence and estimate final biomass.

The hail incident did not lead to a significant change of the correlation coefficient, whereas the start of leaf senescence at 82 DAS until 90 DAS decreased the correlation coefficient between the different measurement points.

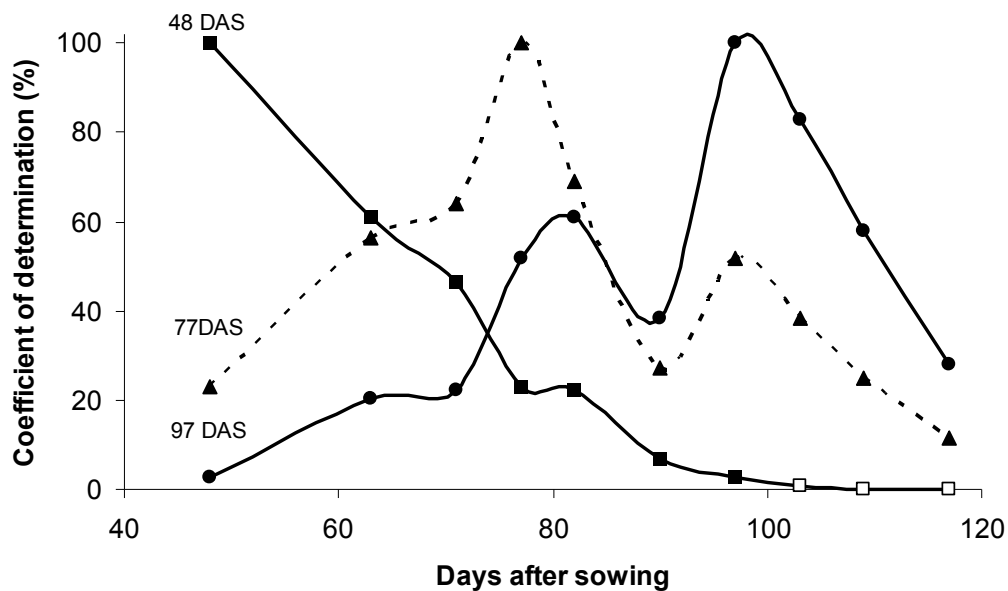
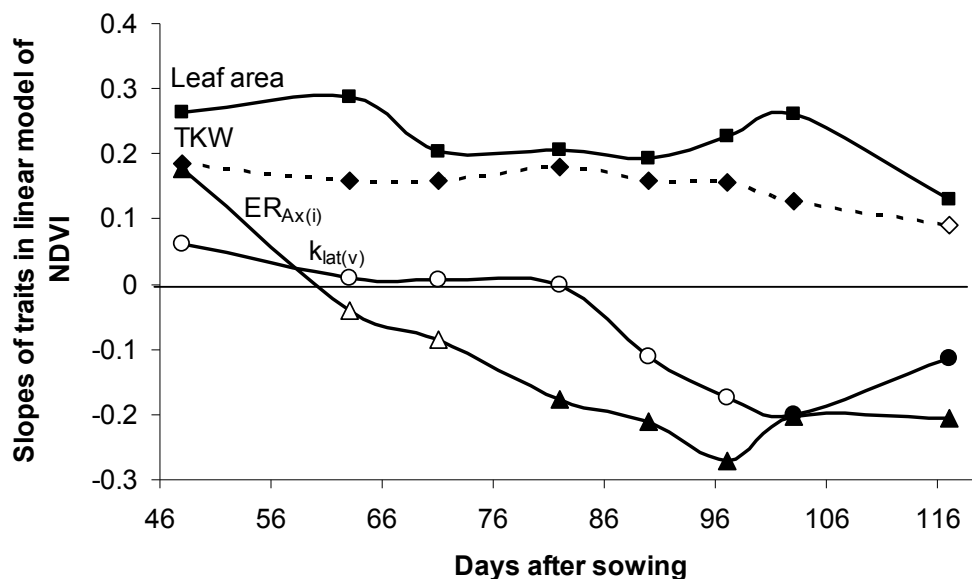


**Figure 9:** Pearson product-moment coefficients of determination of the measurement points 48, 77 and 97 DAS explaining the variation of NDVI over time. Filled symbols indicate significant correlations ( $p < 0.05$ ).

#### **4.7 Root development during heterotrophic stage related positively to early and negatively to late shoot biomass under drought**

A multiple regression was computed to distinguish between seed, leaf and root traits influencing NDVI over time as the most root traits and the NDVI ( $R^2_{48DAS}=0.14^{***}$ ,  $R^2_{97DAS}=0.04^{**}$ ) were positively related to seed size and seed vigor. In the multiple regression the influence of maturity group, TKW, total leaf area, the percentage of germinated seeds, germination index, the number of developed leaves, elongation rate of visible lateral and axile roots as well as the number of axile roots developed in pouches on NDVI over time was tested. The parameters were normalized for the analysis. Only parameters with a significant effect were considered. Leaf area and TKW as well as the elongation rate of lateral and axile roots were traits, measured in the pouches, which affected NDVI in the field most consistently (Figure 10). The TKW and the leaf area always had a positive influence on NDVI. The relationship between axile ( $ER_{Ax(i)}$ ) and lateral ( $k_{lat(v)}$ ) root elongation and the NDVI values depended on the developmental stage: At 48 DAS a significant positive influence on NDVI was observed. Thereafter, this relationship constantly decreased and became significantly negative after 77 DAS. The same pattern was observed for total root length, horizontal root length, DR and  $D_{95}$  (data not shown). The relationship was approved by a positive relationship between the ratio between total leaf area and total root length and late development of shoot biomass. The ratio correlated positively with NDVI 77 DAS ( $r=0.19^*$ ), 82 and 90 DAS ( $r=0.23^{**}$ ), 97 and 103 DAS ( $r=0.36^{***}$ ), 109 DAS ( $r=0.3^{***}$ ) and 117 DAS ( $r=0.19^*$ ).

Given these observations, the hypothesis that increased heterotrophic root growth has a positive influence on the development of shoot biomass under drought later in the season had to be rejected.



Days after sowing	48	63	71	82	90	97	103	117
Adjusted R <sup>2</sup>	0.22	0.14	0.09	0.11	0.11	0.14	0.14	0.04
Multiple R <sup>2</sup>	0.23	0.16	0.11	0.13	0.13	0.16	0.16	0.06
P-value	***	***	***	***	***	***	***	.

**Figure 10:** Slope estimates of standardized (0 mean, 1 standard deviation) TKW (g), leaf area (cm<sup>2</sup>), ER<sub>Ax(i)</sub> (cm d<sup>-1</sup>) k<sub>lat(v)</sub> (cm d<sup>-1</sup>) influencing NDVI. The slopes were the output of a multiple regression. Significant slopes (p<0.05) are indicated by filled symbols. The P-value as well as the adjusted and multiple R<sup>2</sup> of the model with the consistent parameters are shown in the table.

Neither the sum of the horizontal and vertical root length nor the vertical root lengths in the border of the pouch were related to NDVI over time (data not shown). As such the hypothesis that a shallow heterotrophic root system is negatively related to the development of shoot biomass under drought stress was not approved.

#### 4.8 The development of axile roots during autotrophic stage related positively to shoot biomass under drought

Concerning the parameters researched in columns, a significant negative correlation was found between  $ER_{Ax}$  and early development of shoot biomass (48 DAS) in the field (Figure 11). The relationship turned positive after 82 DAS. The same pattern was observed for  $D_{95}$ , the elongation rate of roots and the development of the number of crown roots (data not shown). Though the positive correlation was not significant it indicated a change in the impact of  $ER_{Ax}$  from negative during the early stages to slightly positive during grain filling under drought stress.

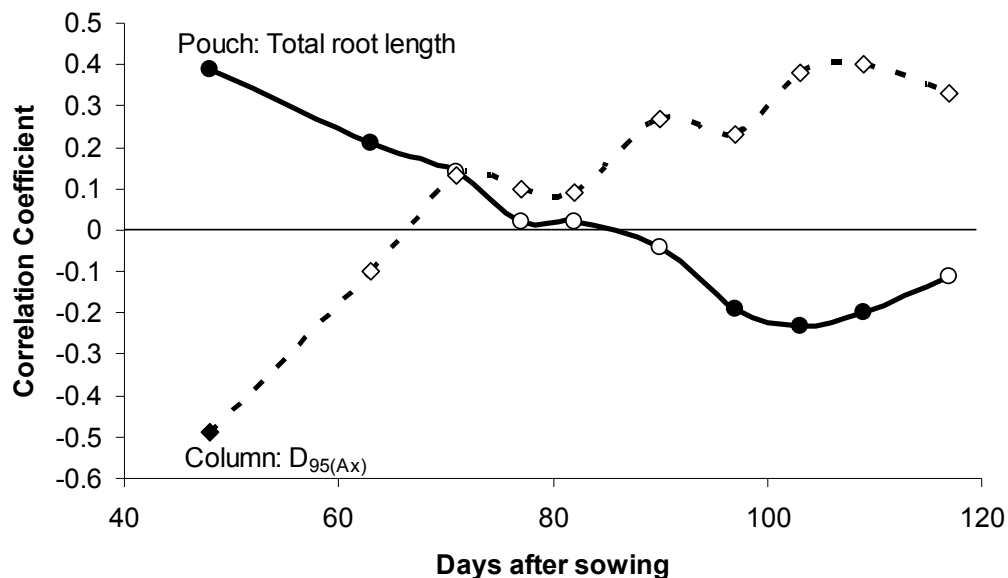
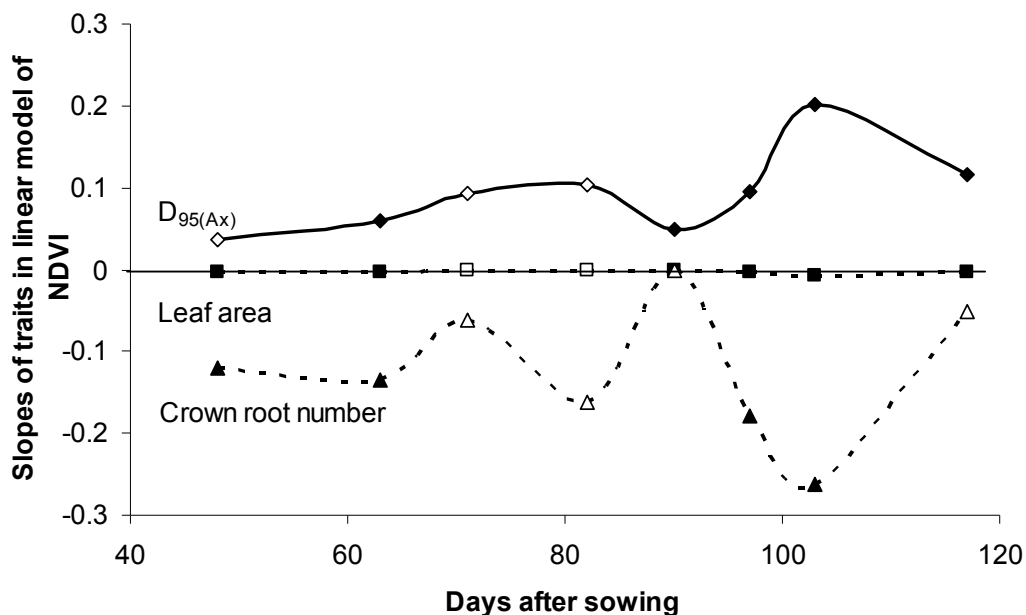


**Figure 11:** Pearson product-moment coefficients between NDVI and total root length (pouch) as well as NDVI and the elongation rate of axile roots ( $D_{95(Ax)}$  Slp; column) in dependence of time. Significant correlations ( $p < 0.05$ ) are indicated with filled symbols.

A multiple regression was computed with the GCP-INRA subset to distinguish between autotrophic leaf and root traits influencing NDVI over time. In the analysis the normalized length at the V2 stage (Int) and development rates between the V2 and V6 stage (Slp) of  $D_{95(Ax)}$ , total root length, DR, number of crown roots, diameter and angle of crown roots as well as the leaf area were included.

The multiple regression showed that the leaf area,  $D_{95(Ax)}$  and the number of crown roots influenced NDVI in the field continuously (Figure 12). The increase of leaf area was slightly negatively related to NDVI over time. The  $D_{95(Ax)}$  was positively related to NDVI, whereas the increase of crown root number negatively related to NDVI over time. The development of root length was less important than the development of root depth indicated by  $D_{95(Ax)}$  as the root length had no significant influence in the linear model on NDVI. In general, less but deeper reaching axile roots, combined with a reduced leaf area seemed to be beneficial for the development of shoot biomass throughout the season. Importantly, their influence increased as the season progressed.



Days after sowing	48	63	71	82	90	97	103	117
Adjusted R <sup>2</sup>	0.21	-0.05	-0.03	-0.11	0.19	0.04	0.31	0.06
Multiple R <sup>2</sup>	0.32	0.09	0.12	0.05	0.31	0.18	0.41	0.2
P-value	0.07	0.59	0.5	0.83	0.08	0.3	0.02	0.25

**Figure 12:** Slope estimates of standardized (0 mean, 1 standard deviation) total leaf area (cm<sup>2</sup>/day),  $D_{95(Ax)}$  (cm d<sup>-1</sup>) and crown root number development influencing NDVI. The slopes were the output of a multiple regression. Significant slopes ( $p < 0.05$ ) are indicated by filled symbols. The P-value as well as the adjusted and multiple R<sup>2</sup> of the model with the consistent parameters are shown in the table.

The relationships between crown root angles (Int and Slp) measured in columns and NDVI were not significant. Nevertheless, the slope of the crown root angle positively correlated with the development of biomass during vegetative growth until 82 DAS (Table 10). By contrast, the intercept of the crown root angle was consistently negatively correlated with NDVI. As a result, a more vertical growth direction of roots emerging from the first crown root tier as well as the maintenance of the roots emerging from successive tiers in a more horizontal growth direction was positively related to the development of shoot biomass until anthesis. As such, the hypothesis that a shallow heterotrophic and autotrophic root system is in general negatively related to the development of shoot biomass under drought stress was not approved.

**Table 10:** Pearson product-moment correlation coefficients of the intercept and slope of crown root angle to the development of shoot biomass over time.

DAS	Crown root angle (°) Int	Crown root angle (°) Slp
48	-0.03	0.29
63	-0.09	0.37
71	-0.31	0.31
77	-0.15	0.34
82	-0.26	0.31
90	-0.01	-0.01
97	-0.13	-0.02
103	-0.2	-0.02
109	-0.17	0.06
117	-0.01	-0.13



## 5 Discussion

### 5.1 Heterotrophic root growth and distribution are best described by the ratio between lateral and axile root length, horizontal root length, $ER_{Ax(i)}$ and $k_{lat(v)}$

The total root length of 1.2 m reached was comparable to the results of Ruta (2008), (1 m) and Trachsel (2009), (1.2 m). 40% of total root length was located in the upper third of the pouch. The total root length was mainly influenced by the growth of axile roots. For most of the genotypes the causal relationship between axile root and lateral root length was observed. The range of axile root and lateral root diameter was consistent with the range of diameters of lateral root of 0.2 to 0.8 mm reported by Varney et al. (1991), even though the system was not calibrated to measure the true diameter of the roots. Seed size and seed vigor proved to influence the root development during heterotrophic stage, but the variation explained by TKW, GI and GP was relatively small.

The elongation rate of individual axile roots ( $ER_{Ax(i)}$ ) was chosen as a parameter to describe the growth of axile roots. The calculation for  $ER_{Ax(i)}$  led to a significant negative relationship with the number of axile roots and axile root index. Thus, the elongation rate of axile roots decreased with increasing number of axile roots. The variation of axile root length explained by  $ER_{Ax}$  decreased from 98% to 73% when only individual axile roots were taken into account. As a result, a genotype with a high number of axile roots does not necessarily have longer axile roots or deeper root system. Thus genotypes with few axile roots but with a deep root system would be underestimated concerning drought tolerance when  $ER_{Ax}$  would be taken into account. As a result the inclusion of  $ER_{Ax(i)}$  improved the interpretation of genotypic root system. The weakness of the new approach for  $ER_{Ax(i)}$  is that the number of axile roots was assigned visually. Thus a discrepancy between the diameter classes measured by WinRhizo and the visible assignment of the number of axile roots could not be excluded. A software detecting individual axile root and tracing them through subsequent images would be the optimal solution to this problem. However, this type of software is not available so far.

The elongation rate of visible lateral roots ( $k_{lat(v)}$ ) was chosen as target parameter to describe the growth of lateral roots. It may provide more reliable information about root morphology than  $k_{lat}$  since it excludes from the model the lag phase until the development of lateral roots. The reason for the greater reliability is that the lag phase may be greatly influenced by differences in germination. Differences in germination may lead to errors in determining the true growth of lateral roots, if measured at one point in time only (Hund et al. 2009b). Disregarding different lag phases may have a similar effect on  $k_{Lat}$ . However,  $k_{lat(v)}$  had a lower heritability and a lower correlation to the lateral root length at the end of the experiment compared to  $k_{lat}$ . This may be explained by the fact that  $k_{lat}$  combines both intrinsic differences in germination and the growth of lateral roots among lines. Both factors may lead to an apparently greater heritability of  $k_{lat}$ .

Although  $D_{95}$  was defined in pouches, the heritability of this trait was higher compared to DR. As such,  $D_{95}$  is the best parameter for describing rooting depth. In total, the ratio between lateral and axile root length as well as  $k_{lat(v)}$ ,  $ER_{Ax(l)}$  and  $D_{95}$  can be used to characterize genotypes according to their root system, root development and rooting depth, respectively.

A new method was established for characterizing genotypes concerning their root distribution on the surface of the pouch. The genotypes could be characterized by the proportion of vertical (border of the pouch) and horizontal growing roots (upper third of the pouch) concerning their root distribution. The parameters can further be used to estimate seminal root angle as it was shown that a high horizontal and vertical root length lead to an increased root distribution on the surface of the blotting paper.

## **5.2 Root growth parameters assessed during heterotrophic stage explained 20% of the root development during autotrophic stage**

The heterotrophic total and axile root length as well as the  $D_{95}$  and DR at the V2 stage measured in pouches and columns were not significantly related. This might be due to various factors: I) The seeds used in columns and pouches originated from different seed stocks. The TKW of the two stocks did not correlate ( $r=0.15$ ) and TKW was thus not heritable. Since seed size had a certain influence on the different root traits at the V2 stage, the lack of correlation between heterotrophic and autotrophic root traits is not surprising. II) The different means used to measure root traits (WinRhizo vs. root staining) have different precision that may have led to an increased random variation. III) The different growth substrates (blotting paper vs. sand-Seramis™ mixture) may have led to a certain degree of genotype-environment interaction.

Further, only 18% of the variation in the elongation rate of the roots between the V2 and the V6 stage in columns could be explained by the total root length reached in pouches. Root length and root development measured in pouches were not significantly correlated to the development of crown roots in columns. Thus, the variation not explained by heterotrophic root growth could be the variation of the development of crown roots.

The DR measured in pouches was negatively related to the angle of the crown roots from the first tier measured in columns. In total, DR explained 27% of the variation of crown root angle. As a consequence, a larger root angle was related to a greater proportion of roots in the upper half of the root system. However, the heritability of DR was low and, thus, indirect selection for crown root angle with this parameter might not be reliable. The root angle indicated by root distribution (vertical root length, horizontal root length and the sum of both parameters) was not related to crown root angle. This might be influenced by the fact, that in the pouch the seminal root angle was indirectly measured by vertical root length, whereas the root angle in columns was measured for the crown roots.

Hund (unpublished) showed, for a set of 9 divergent inbred lines that the angle of the seminal roots can predict up to 70% of the variation in the crown root angles of the successive two crown root tiers. Araki et al. (2000) showed that, for the maize variety Robust, the rooting angle decreased as the rooting nodes advanced, i.e. roots from later developed nodes had a more vertical inclination. According to Manschadi et al. (2008) wheat root system architecture is linked to the angle of seminal root axes at the seedling stage. As a result, the heritability of seminal and crown root angle should be high. To research the seminal or crown root angle in pouches directly a new software should be programmed, which enables the measurement of root length and root diameter between specific parts of the root system.

### **5.3 Operation efficiency of the photosystem II ( $\Phi_{PSII}$ ) measured in pouches related to the root development during autotrophic stage**

Surprisingly  $\Phi_{PSII}$  (measured in the pouches) and elongation rate of roots (measured in the columns) were strongly related ( $R^2=0.66$ ). The positive relationship between  $\Phi_{PSII}$  and heterotrophic and autotrophic root parameters suggested that a strong photosynthetic performance is important for vigorous early growth between V2 and the V6 stage. The positive relationship between  $\Phi_{PSII}$  and root length was higher than the relationship between different root traits and thus is an interesting parameter to measure during early plant development. Concerning this rather strong influence of photosynthetic performance, it has to be considered that differences in photosynthesis may strongly influence plant performance even under close-to-optimum conditions. Modern temperate inbred lines do usually not differ for  $\Phi_{PSII}$  under these conditions but differ for example under cold stress (Fracheboud et al. 1999, Hund et al. 2008). It may be argued that due to its artificial conditions, the pouch system imposes stress on the plants, leading to segregation of inbred lines for  $\Phi_{PSII}$ . However, Reimer (unpublished) did not find such differences when modern temperate inbred lines were grown in pouches under close-to-optimal conditions. This suggests the presence of constitutive differences in photosynthetic performance among inbred lines.

Therefore, it would be advisable to test the GCP-INRA set again at a later stage of development in order to verify the results. Eventually, photosynthetic performance under close-to-optimum conditions may be used as a cofactor to prove the predictive value of root characteristics for shoot biomass in the field.

#### **5.4 NDVI precision was sensitive to plant density**

The precision of NDVI could be improved by taking only the plots with more than 50% plant density into account. The reasons for a decreased precision of NDVI in plots with low plant density were the seed quality (TKW) and seed vigor (germination index and the percentage of germinated seeds). Seed quality and seed vigor affected the percentage of emergence which can influence grain yield by altering plant population density, spatial arrangement and crop duration (Ellis et al. 1992). As a result TKW, GI and GP influenced plant density and the precision of NDVI in plots with a low plant density. This was evidenced by a positive correlation of plot plant density with NDVI values. The problem of an uneven plant stand on the NDVI data was already emphasized in Huete (1988). The development of shoot biomass increased until flowering followed by senescence. With NDVI the plant biomass could be depicted, as it was positively correlated to the number of plants harvested, which approved the results of Marti et al. (2007). A measurement at 48 DAS can be used to assess early shoot biomass. A measurement at 77 DAS can be used to assess the development of shoot biomass until and during flowering. A measurement at 97 DAS can be used to estimate leaf senescence and final shoot biomass.

## **5.5 Heterotrophic $ER_{Ax(i)}$ , $k_{lat}$ and horizontal root length related negatively related to late shoot biomass under drought**

Hypothesis I was not verified: A greater proliferation of axile roots in the pouch system did not lead to a better plant performance later in the field under drought stress. Heterotrophic  $ER_{Ax(i)}$  was positively related to early development of shoot biomass in the field which showed the importance of early heterotrophic root growth for plant establishment. Late development of shoot biomass was negatively related to  $ER_{Ax(i)}$  and  $k_{lat}$ . Horizontal root length, DR and  $D_{95}$  showed, like  $ER_{Ax(i)}$  and  $k_{lat(v)}$ , a positive relationship to early biomass and a negative relationship to later development shoot biomass under drought. Thus, the total root length as well as root distribution and rooting depth were negatively related to shoot biomass under drought stress.  $ER_{Ax(i)}$  could maximally explain 10% of NDVI development over time. The separation of total root lengths into lateral and axile root length did not improve the relationship with NDVI over time. According to Hund et al. (2009b) genotypes with a prolific growth of axile roots during the heterotrophic growth stage should be more drought tolerant than genotypes with more prolific development of lateral roots. This relationship could not be approved in the current study. The relationship of lateral and axile elongation rate to NDVI should be evaluated under control conditions to approve the negative relationship to the development of shoot biomass. Further research of the elongation rate of different axile roots would improve the interpretation.

The ratio between leaf area and total root length approved the negative relationship between heterotrophic root length and the development of shoot biomass under drought, even though the ratio showed the positive relationship of early leaf area to later the development of shoot biomass. The ratio between leaf area and total root length was the only parameter measured in pouches, which was not correlated with seed quality or seed vigor but explained maximum 13% of late NDVI variation. As such, this ratio was the most reliable parameter measured in pouches to evaluate late development of shoot biomass and leaf senescence under drought stress.

In total, the data suggest that a general decrease in root vigor may be beneficial for later stages of development. This observation is consistent with the observation of Sanguineti et al. (2006), who stated that increases in plant density may have favored the selection of hybrids with less vigorous root systems in the early growth stages. The less vigorous root system would delay the onset of competition among adjacent plants for soil nutrients and water and contribute to optimize their use. In an unpublished study of Barker and Saab (mentioned in Bruce et al. 2002) inbred lines with a poorer early root development yielded better than the lines with more vigorous root development. The authors concluded that vigorous root growth may come at cost to grain production despite the advantage for water acquisition in dry soils. However, as outlined in the introduction, an increasing number of studies exist claiming a positive effect of the growth of axile roots at early developmental stages that can be positively attributed to plant performance during later stages.

The negative influence of heterotrophic root growth on the development of shoot biomass under drought might be further explained by the fact that the water uptake of the seminal and primary root goes through the mesocotyl (Cahn 1989). If the mesocotyl is damaged by insects or a fungus, the water supply would decrease to a high extent. Nevertheless, a vigorous heterotrophic root growth is important for seed establishment influencing plant density as discussed above. To further approve these relationships, the same analysis has to be carried out with the well watered treatment.

Also the Hypothesis II could not be verified: A more vertical orientation of the roots in the pouches was not significantly related to late the development of shoot biomass under drought stress. Araki et al. (2000) stated that the root angle of the seminal roots was relatively large, approximately 50 degrees (Araki et al. 2000). The large root angle of seminal roots measured by Araki et al. (2000) might be positive for nutrient and water acquisition in the upper part of the soil. Bonser et al. (1996), Lynch et al. (2001) and Liao et al. (2004) found that the growth angle of bean seedlings correlated with field performance in low P soils. Thus, a higher seminal growth angle should lead to increased topsoil foraging during early developmental stages.

Nevertheless, increased P uptake of the seminal root system did not lead to a significant relationship to early the development of shoot biomass in the field.

### **5.6 Autotrophic axile elongation rate positively related to shoot biomass under drought**

The development of  $D_{95(Ax)}$  in growth columns, which can be viewed as the growth rates of axile roots to greater depth, increased shoot biomass acquisition in the field. Thus, contrary to the results observed in pouches, this result is approved hypothesis I. Importantly, the  $D_{95(Ax)}$  at the V2 stage could not explain shoot biomass accumulation in the field. This raises the question if the higher throughput of measuring the root system at early developmental stages really outbalances the lower precision. This lower precision is surely related to the fact that only the embryonic root system can be measured and the plants still rely on seed reserve. The measurement between the V2 and V6 stage offer two advantages: the autotrophic development can be assessed and the development of the shoot-borne crown roots can be measured. The crown roots form the major part of the adult root system (Mc Cully 1999). Furthermore, crown roots forward the water directly to the xylem vessels of the shoot while the water of the embryonic root system has to pass through the narrow mesocotyle. The number of crown roots developed had a negative influence on the development of shoot biomass over time. Bruce et al. (2002) showed for recombinant inbred lines that poor early root development is connected with reduced the development of crown roots and increased yield potential under drought stress. Thus a low crown root number at early autotrophic growth stage can be used to select for genotypes adapted to drought prone environments.

The crown root angle did not significantly correlate with the development of shoot biomass in the field. However, the maintenance of the roots emerging from successive tiers in a more horizontal growth direction was positively related to the development of shoot biomass until anthesis. This greater benefit of shallower rooting during drought stress may be related to better nutrient availability, due to top-soil foraging similar to what was observed for common bean in phosphorus poor soils (Bonser et al. 1996).



This raises the question if increased top soil foraging outbalances deeper rooting. In conclusion, the knowledge about the target soil environment and the type of stress may greatly enhance the understanding of the benefits from altered root angles (Ho et al. 2005). In the present study, an increased number of field experiments with well characterized soil parameters may improve the understanding of the benefits of different root angles.

## **6 Conclusion**

The study aimed to elucidate the predictive value of root traits measured at the seedling stage in pouches under well watered conditions. One specific question was if an early increase in growth and vertical orientation of axile roots could be predictive for later stages of development and, consequently, for drought avoidance in the field.

The results suggest that early heterotrophic root growth is necessary for successful plant establishment but explained a low proportion of variation of root architecture at later stages. Nevertheless the genetic variation of the root length in the upper third of the pouch (horizontal root length) as well as the elongation rate of individual axile roots ( $ER_{Ax(i)}$ ) and visible lateral roots ( $k_{lat(v)}$ ) can be used to select genotypes with a good root development during heterotrophic stage. These genotypes should be further observed during the early root development during autotrophic stage, as accelerated growth of the root system to greater soil depth is essential for the development of shoot biomass under drought. With some investment in the pouch system, it should be possible to map QTLs for root architecture even beyond the V2 stage. This would greatly enhance our understanding of the inheritance of root architecture, which is related to water and nutrient uptake from the soil. For this, bigger pouches of at least 50x80 cm need to be used to phenotype a sufficient amount of genotypes during the early autotrophic root growth. The development of this system is in progress.

## 7 References

- Araki, H., M. Hirayama, et al. (2000). "Which Roots Penetrate the Deepest in Rice and Maize Root Systems?" *Plant Prod. Sci.* 3(3): 281-288.
- Babu, R. C., M. S. Pathan, et al. (1999). "Comparison of Measurement Methods of Osmotic Adjustment in Rice Cultivars." *Crop Sci* 39: 150-158.
- Bänziger, M., S. Mugo, et al. (1999). "Breeding for Drought Tolerance in Tropical Maize - Conventional Approaches and Challenges to Molecular Approaches." Retrieved 20.10.2008, from [www.cimmyt.org](http://www.cimmyt.org).
- Böhm, W. (1979). *Methods of Studying Root Systems*. W. D. Billings, F. Golley, O. L. Lange and J. S. Olson. Berlin, Heidelberg, New York, Springer Verlag: 4, 5, 13, 20, 29.
- Bolaños, J. and G. O. Edmeades (1993). "Eight cycles of selection for drought tolerance in lowland tropical maize. I. Responses in grain yield, biomass, and radiation utilization." *Field Crops Research* 31: 233-252.
- Bolaños, J. and G. O. Edmeades (1996). "The importance of the anthesis-silking interval in breeding for drought tolerance in tropical maize." *Field Crops Research* 48(1): 65-80.
- Bolaños, J., G. O. Edmeades, et al. (1993). "Eight cycles of selection for drought tolerance in lowland tropical maize. III. Responses in drought-adaptive physiological and morphological traits." *Field Crops Research* 31: 269-286.
- Bonser, A. M., J. Lynch, et al. (1996). "Effect of phosphorus deficiency on growth angle of basal roots in *Phaseolus vulgaris*." *New Phytologist* 132(2): 281-288.
- Boyer, J. S. and M. E. Westgate (2004). "Grain yields with limited water." *Journal of Experimental Botany* 55(407): 2385-2394.
- Bruce, W. B., G. O. Edmeades, et al. (2002). "Molecular and physiological approaches to maize improvement for drought tolerance." *Journal of Experimental Botany* 53(366): 13-25.
- Butler, D. (2006). *asreml:asreml() fits the linear mixed model*, R package version 2.00.
- Cahn, M. D., R. W. Zobel, et al. (1989). "Relationship between root elongation rate and diameter and duration of growth of lateral roots of maize." *Plant and Soil* 119(2): 271-279.
- Calvo, R., F. Carión, et al. (1999). *CIMMYT 1997/98 World Maize Facts and Trends; Maize Production in Drought-Stressed Environments: Technical Options and Research Resource Allocation. The World Maize Economy: Current Issues*. CIMMYT. Mexico: 37-40.
- Camacho, R. G. and D. F. Caraballo (1994). "Evaluation of Morphological Characteristics in Venezuelan Maize (*Zea mays* L.) Genotypes under Drought Stress." *Sci. agric., Piracicaba* 51(3): 453-458.
- Campos, H., M. Cooper, et al. (2004). "Improving drought tolerance in maize: a view from industry." *Field Crops Research* 90: 19-34.
- Cutforth, H. W., C. F. Shaykewich, et al. (1986). "Effect of Soil Water and Temperature on Corn (*Zea Mays* L.) Root Growth during Emergence." *Can. J. Soil Sci.* 66: 51-58.
- Edmeades, G. O., J. Bolaños, et al. (1999). "Selection improves drought tolerance in tropical maize populations: I. Gains in biomass, grain yield, and harvest index." *Crop Science* 39(5): 1306-1315.
- Eghball, B., J. R. Settimi, et al. (1993). "Fractal analysis for morphological description of corn roots under nitrogen stress." *Agronomy Journal* 85(2): 287-289.
- Ellis, R. H. (1992). "Seed and seedling vigor in relation to crop growth and yield." *Plant Growth Regulation* 11: 249-255.

- Enns, L. C., M. E. McCully, et al. (2006). "Branch roots of young maize seedlings, their production, growth, and phloem supply from the primary root." *Functional Plant Biology* 33(4): 391-399.
- FAO. (2003). "The State of Food Insecurity in the world 2003. Monitoring Progress towards the World Food Summit and Millennium Development Goals." Retrieved 19.01.2009, from <ftp://ftp.fao.org/>.
- FAO. (2008). "The State of Food Insecurity in the World. High food prices and food security – threats and opportunities." Retrieved 16.12.2008, from <ftp://ftp.fao.org/>.
- Fracheboud, Y., P. Haldimann, et al. (1999). "Chlorophyll fluorescence as a selection tool for cold tolerance of photosynthesis in maize (*Zea mays* L.)." *Journal of Experimental Botany* 50(338): 1533-1540.
- Govaerts, B., N. Verhulst, et al. (2007). "Evaluating spatial within plot crop variability for different management practices with an optical sensor?" *Plant Soil* 299: 29–42.
- Grieder, C. (2008). Depth and vertical distribution of roots: Variation within a diverse panel of tropical maize inbred lines. Agronomy and Plant breeding, ETH Zurich. Master of Science.
- Hammer, G. L., Z. Dong, et al. (2009). "Can Changes in Canopy and/or Root System Architecture Explain Historical Maize Yield Trends in the U.S. Corn Belt?" *Crop Science* 49.
- Hill, J. H. (2007). How a Corn Plant Develops - Identifying Stages of Development, Iowa State University.
- Ho, M. D., J. C. Rosas, et al. (2005). "Root architectural tradeoffs for water and phosphorus acquisition." *Functional Plant Biology* 32(8): 737-748.
- Hoagland, D. R. and D. I. Arnon (1938). The water-culture method for growing plants without soil. Berkeley, California Agricultural Experiment Station.
- Hochholdinger, F., K. Woll, et al. (2004). "Genetic Dissection of Root Formation in Maize (*Zea mays*) Reveals Root-type Specific Developmental Programs." *Annals of Botany* 93(4): 359-368.
- Huete, A. R. (1988). "A Soil-Adjusted Vegetation Index (SAVI)." *Remote Sensing of Environment* 25: 295-309.
- Hund, A., Y. Fracheboud, et al. (2004). "QTL controlling root and shoot traits of maize seedlings under cold stress." *Theoretical and Applied Genetics* 109(3): 618-629.
- Hund, A., Y. Fracheboud, et al. (2008). "Cold tolerance of maize seedlings as determined by root morphology and photosynthetic traits." *European Journal of Agronomy* 28(3): 178-185.
- Hund, A., W. Richner, et al. (2007). "Root morphology and photosynthetic performance of maize inbred lines at low temperature." *European Journal of Agronomy* 27(1): 52-61.
- Hund, A., N. Ruta, et al. (2009a). "Rooting depth and water use efficiency of tropical maize inbred lines, differing in drought tolerance." *Plant and Soil* 318(1-2): 311-325.
- Hund, A., S. Trachsel, et al. (2009b). "Growth of axile and lateral roots of maize: I. Development of a phenotyping platform." *Plant and Soil* (DOI: 10.1007/s11104-009-9984-2 ).
- Inman, D., R. Khosla, et al. (2008). "Normalized Difference Vegetation Index and Soil Color-Based Management Zones in Irrigated Maize." *Agronomy Journal* 100(1): 60-66.
- Inman, D., R. Khosla, et al. (2007). "Active remote sensing and grain yield in irrigated maize." *Precision Agric* 8: 241–252.
- Ito, K., K. Tanakamaru, et al. (2006). "Lateral root development, including responses to soil drying, of maize (*Zea mays*) and wheat (*Triticum aestivum*) seminal roots." *Physiologia Plantarum* 127(2): 260-267.

- Liao, H., X. L. Yan, et al. (2004). "Genetic mapping of basal root gravitropism and phosphorus acquisition efficiency in common bean." *Functional Plant Biology* 31(10): 959-970.
- Liedgens, M., A. Soldati, et al. (2000). "Root Development of Maize (*Zea mays* L.) as Observed with Minirhizoctrons in Lysimeters." *Crop Science* 40: 1665-1672.
- Lynch, J. (1995). "Root Architecture and Plant Productivity." *Plant Physiology* 109(1): 7-13.
- Lynch, J. P. and K. M. Brown (2001). "Topsoil foraging - an architectural adaptation of plants to low phosphorus availability." *Plant and Soil* 237: 225-237.
- Manschadi, A. M., J. Christopher, et al. (2006). "The role of root architectural traits in adaptation of wheat to water-limited environments." *Functional Plant Biology* 33: 823-837.
- Marti, J., J. Bort, et al. (2007). "Can wheat yield be assessed by early measurements of Normalized Difference Vegetation Index?" *Ann Appl Biol* 150: 253-257.
- McCully, M. (1999). "ROOTS IN SOIL: Unearthing the Complexities of Roots and Their Rhizospheres." *Annu. Rev. Plant Physiol. Plant Mol. Biol.* 50: 695-718.
- McCully, M. E. and M. J. Canny (1988). "Pathways and Processes of Water and Nutrient Movements in Roots." *Plant and Soil* 111(2): 159-170.
- Monneveux, P., C. Sánchez, et al. (2005). "Drought Tolerance Improvement in Tropical Maize Source Populations: Evidence of Progress." *Crop Science* 46: 180-191.
- Monneveux, P., C. Sanchez, et al. (2008). "Future progress in drought tolerance in maize needs new secondary traits and cross combinations." *Journal of Agricultural Science* 146: 287-300.
- Ohdan, H., H. Daimon, et al. (1995). "Evaluation of Allelopathy in *Crotalaria* by Using a Seed Pack Growth Pouch." *Jpn. J. Crop. Sci.* 64(3): 644-649.
- Ruta, N. (2008). Quantitative Trait Loci controlling Root and Shoot traits of Maize under Drought Stress. Zurich, ETH Zurich. Doctor of Science.
- Ruta, N., M. Liedgens, et al. (2009). QTLs for the elongation rates of drought affected axile and lateral maize roots. *Plant and Soil*, Manuscript.
- Sanguineti, M. C., D. N. Duvick, et al. (2005). "Effects of long-term selection on seedling traits and ABA accumulation in commercial maize hybrids." *Maydica* 51: 329-338.
- Schmidhalter, U., M. Evequoz, et al. (1998). "Sequence of drought response of maize seedlings in drying soil." *Physiologia Plantarum* 104(2): 159-168.
- Smith, S. D. and A. H. Millet (1964). "Germination and sprouting responses of the tomato at low temperature." *Proc. Am. Soc. Hortic. Sci.* 84(480-484).
- Teal, R. K., B. Tubana, et al. (2006). "In-Season Prediction of Corn Grain Yield Potential Using Normalized Difference Vegetation Index." *Agron* 98: 1488-1494.
- Tollenaar, M. and J. Wu (1999). "Yield improvement in temperate maize is attributable to greater stress tolerance." *Crop Science* 39(6): 1597-1604.
- Trachsel, S. (2009). Genetic analysis of root morphology and growth of tropical maize and their role in tolerance to desiccation, aluminum toxicity and high temperature, ETH Zurich. Doctor of Sciences.
- Varney, G. T., M. J. Canny, et al. (1991). "The Branch Roots of *Zea*. I. First Order Branches, Their Number, Sizes and Division Into Classes." *Annals of Botany* 67: 357-364.

## 8 Appendix

**A 1:** Macro programmed in Image J for inverting a colored picture to a black (background) and white (root) image.

```
dir1 = getDirectory("Choose Source Directory ");
dir2 = getDirectory("Choose Destination Directory ");
list = getFileList(dir1);
//setBatchMode(true);
for (i=0; i<list.length; i++) {
    showProgress(i+1, list.length);
    open(dir1+list[i]);
//Crop image to omit pouch borders
    makeRectangle(144, 360, 4764, 6660);
    run("Crop");
    run("HSB Stack");
    IMG1= getImageID();
//Use only the hue channel (IMG3)
    run("Duplicate...", "title=IMG3.jpg");
    IMG3= getImageID();
//Use only the saturation channel (IMG1)
    selectImage(IMG1);
    run("Delete Slice");
    IMG1= getImageID();
//Prepare values image (IMG2)
    run("Next Slice [>]");
    run("Duplicate...", "title=IMG2.jpg");
    IMG2= getImageID();
//Process saturation image (IMG1)
    selectImage(IMG1);
    run("Delete Slice");
    run("Image Inverter");
    //Remove noise
        run("Gaussian Blur...", "sigma=3");
    //Apply threshold
        setThreshold(191, 255);
        run("Convert to Mask");
//Process value image (IMG2) (This filter detects the black pouch)
    selectImage(IMG2);
    setThreshold(66, 255);
    run("Convert to Mask");
//Process hue image (IMG3) (This filter detects the colored seed)
    selectImage(IMG3);
    setThreshold(50, 48);
    run("Convert to Mask", " ");
    //Invert
        run("Image Inverter");
    //Binary increase seed
        run("Erode");
//Add images
    //Saturation times value
    imageCalculator ("Multiply", IMG1, IMG2);
```

```

        //Saturation times hue
        imageCalculator ("Multiply", IMG1, IMG3);
//Binary remove root hairs
        //run("Options...", "iterations=2 count=4");
        selectImage(IMG1);
        saveAs("Jpeg", dir2+list[i]);
        close();
        close();
        close();
}

```

**A 2** Macro programmed in Image J for selecting and saving horizontal and vertical parts of the image

```

        dir1 = getDirectory("Choose Source Directory ");
        dir2 = getDirectory("Choose Destination Directory ");
        list = getFileList(dir1);
        //setBatchMode(true);
for (i=0; i<list.length; i++) {
        showProgress(i+1, list.length);
        open(dir1+list[i]);
//Left third down (vertical root length at the left border)
        makeRectangle(0, 0, 1588, 6660);
        run("Duplicate...", "title=.jpg");
        NewName=replace(list[i], ".jpg", "-1-left-down.jpg");
        saveAs("Jpeg", dir2+NewName);
        close();
//Right third down (vertical root length at the right border)
        makeRectangle(3176, 0, 1588, 6660);
        run("Duplicate...", "title=.jpg");
        NewName=replace(list[i], ".jpg", "-3-right-down.jpg");
        saveAs("Jpeg", dir2+NewName);
        close();
//Upper third across (horizontal root length; vertical root growth)
        makeRectangle(0, 0, 4764, 2220);
        run("Duplicate...", "title=.jpg");
        NewName=replace(list[i], ".jpg", "-4-top-across.jpg");
        saveAs("Jpeg", dir2+NewName);
        close();
//Middle third across (vertical root growth)
        makeRectangle(0, 2220, 4764, 2220);
        run("Duplicate...", "title=.jpg");
        NewName=replace(list[i], ".jpg", "-5-middle-across.jpg");
        saveAs("Jpeg", dir2+NewName);
        close();
//Lower third across (vertical root growth)
        makeRectangle(0, 4440, 4764, 2220);
        run("Duplicate...", "title=.jpg");
        NewName=replace(list[i], ".jpg", "-6-down-across.jpg");
        saveAs("Jpeg", dir2+NewName);
        close();
        close();
}

```

## **Affirmation**

I hereby declare that the following master thesis "Is seedling root architecture related to the development of shoot biomass in the field under drought? Lessons learned from a reference set of 226 maize inbred lines" has been written only by the undersigned and without any assistance from third parties. This thesis has not been presented to any other examination board in this or a similar form. Furthermore, I confirm that no sources have been used in the preparation of this thesis other than those indicated in the thesis itself. Thoughts that were taken directly or indirectly from other sources are indicated as such.

---

Zurich, 22. July 2009